

**Gut microbiota transmission prevents antibiotic-induced stochastic loss of
colonization resistance**

Rita A. Oliveira¹, Katharine M. Ng², Margarida B. Correia¹, Vitor Cabral¹, Handuo Shi², Justin
L. Sonnenburg^{3,4}, Kerwyn Casey Huang^{2,3,4}, Karina B. Xavier^{1,*}

¹Instituto Gulbenkian de Ciência, Oeiras, Portugal

²Department of Bioengineering, Stanford University School of Medicine, Stanford, CA
94305, USA

³Department of Microbiology & Immunology, Stanford University School of Medicine,
Stanford, CA 94305, USA

⁴Chan Zuckerberg Biohub, San Francisco, CA 94158, USA

*Corresponding author: kxavier@igc.gulbenkian.pt

Keywords: *Escherichia coli*, *Klebsiella michiganensis*, *Salmonella* Typhimurium,
Proteobacteria, streptomycin, ciprofloxacin, housing, gamma diversity, nutrient
competition, microbiota, dysbiosis

Abstract

The intestinal microbiota contains beneficial microorganisms that protect against pathogen colonization. Antibiotics can disrupt the microbiota and compromise colonization resistance. Here, we determine how the exchange of microbes between hosts impacts the resilience of the gut microbiota to resist colonization after antibiotic-induced dysbiosis. We assess the functional consequences of dysbiosis using a mouse model of colonization resistance against an invading *Escherichia coli*. Antibiotics caused the stochastic loss of microbiota members, but the microbiotas of co-housed animals remained more similar to each other than those among singly housed animals. Strikingly, co-housed animals maintained colonization resistance after antibiotics, whereas most singly housed mice were susceptible to invasion by *E. coli*. The ability to retain or share a particular commensal, *Klebsiella michiganensis*, a related member of the same family Enterobacteriaceae, was sufficient for colonization resistance after antibiotic-induced dysbiosis. *K. michiganensis* generally outcompeted *E. coli in vitro*, but *in vivo* administration of galactitol to bi-colonized gnotobiotic mice, a nutrient that supports only *E. coli* growth *in vitro*, abolished the colonization resistance capacity of *K. michiganensis* against *E. coli*, supporting nutrient competition as the primary mechanism for their interaction. *K. michiganensis* also hampered colonization of the enteric Enterobacteriaceae pathogen *Salmonella enterica* serovar Typhimurium and prolonged host survival. Our results address the functional consequences of the stochastic effects of antibiotic treatments, whereby microbial transmission through host interactions can facilitate the reacquisition of beneficial commensals and thus minimize the negative impact of antibiotics.

Introduction

Mammals rely on their microbiome to be healthy. The intestinal microbiome is essential for host nutrition and immunity¹⁻³, and to resist pathogen colonization and pathobiont expansion⁴⁻⁶. This microbial consortium is initially acquired at birth, and is thereafter affected by the environment and undergoes changes post-weaning until adulthood⁷. In humans, diverse gut microbiotas can be highly stable⁸, but strong differences in diet, lifestyle, host genotype, and drug treatments—especially antibiotics—are robust determinants of microbiota composition⁹⁻¹². Antibiotics are lifesaving therapies against bacterial pathogens. However, their administration can kill commensal gut microbes and increase host susceptibility to a wide range of bacterial infections¹³⁻¹⁶. Antibiotics can lead to intestinal expansion by unwanted bacteria, such as certain members of the Enterobacteriaceae and Enterococcaceae families, and compromise the ability of hosts to inhibit their expansion—a phenomenon called “colonization resistance”^{17,18}.

Molecular mechanisms involved in colonization resistance by microbiota members have been identified in some cases against particular species or taxonomic groups, such as Proteobacteria (e.g. from the Enterobacteriaceae family *Escherichia* and *Salmonella* in particular) and Firmicutes (e.g. *Clostridia*)^{4,19}. These known mechanisms of colonization resistance mainly involve (1) metabolic processes²⁰, involving competition for nutritional niches²¹⁻²⁴; (2) production of inhibitory or signaling molecules²⁵⁻³³; and (3) contact-dependent killing^{34,35}. Antibiotics disrupt the microbiota and potentially affect all of these mechanisms, possibly accounting for the breakdown of colonization resistance against

intestinal pathogens. Identification of environmental factors that minimize loss of protective bacteria upon perturbations can facilitate the development of general strategies to attenuate the negative impact of antibiotics and other drugs.

In the gut, competition for nutrients is highly shaped by diet and cross-feeding among established species, to optimize the available resources^{36,37}. This competition poses a challenge for invading species, since unutilized niches are unlikely to exist. Dietary fiber and mucus polysaccharides are mostly degraded by strict anaerobes, and the released di- and mono-saccharides are rapidly taken up by other commensals, including Enterobacteriaceae species³⁸. One such Enterobacteriaceae species, *Escherichia coli*, efficiently consumes simple sugars present in the mucus layer, such as fucose, mannose, and arabinose³⁸. On average, five different commensal *E. coli* strains are able to co-exist in the gut, with subtle differences in their sugar utilization repertoires³⁹. These commensals are important to successfully ensure colonization resistance to pathogenic *E. coli*^{22,39}. It is unknown whether other commensal species also confer colonization resistance to *E. coli* through competition for nutrients, such as more efficient carbon source utilization.

Transmission and re-inoculation are processes that, by promoting maintenance of commensal microbes, can potentially play an important role in the resilience capacity of the microbiota and its ability to mount resistance against invasion⁴⁰. Evidence that transmission efficacy relies on the level of inter-host interactions is supported by data from both mice⁴¹ and cohabiting humans⁴², despite the uniqueness of coprophagic behavior to mice. During a perturbation such as antibiotic treatment, transmission may play an even

more critical role in re-colonization of important species that are stochastically eliminated. The possibility of re-acquisition of these species relies on their presence within the environmental microbial reservoir, and hence can depend on the degree of interactions among hosts^{43,44}; isolated hosts would have to rely only on their own microbial reservoir that survived the treatment. Despite this seemingly obvious importance, the functional consequences of preventing interactions between hosts have been underexplored.

Here, to interrogate the effect of the presence or absence of multiple hosts in the resilience capacity of the microbiota, we studied the effect of antibiotics in a laboratory mouse population under different housing conditions. We observed that the aggregate microbiota reservoir in co-housed animals resulted in increased colonization resistance capacity after antibiotic-induced dysbiosis versus singly housed animals. Antibiotic treatment of mice singly housed in different cages had stochastic effects on gut microbiota composition, that were particularly striking among members of the Proteobacteria, with loss of all members of this phylum in ~50% of singly housed mice. In mice sharing the same cage (co-housed), all were able to maintain Proteobacteria, indicating that its stochastic extinction is attenuated by the environmental reservoir. We identified a member of the microbiota belonging to the Proteobacteria phylum (*Klebsiella michiganensis*) that was sufficient for colonization resistance against an invading *E. coli*. *K. michiganensis* and *E. coli* are related members of the family Enterobacteriaceae, and we show that nutritional competition plays a key role in the inhibition of *E. coli* by *K. michiganensis*. Moreover, *K. michiganensis* also delayed colonization of the enteric Enterobacteriaceae pathogen *Salmonella enterica* serovar Typhimurium, prolonging host survival. Our results demonstrate the importance of

110 interactions among hosts to the shared microbial reservoir and their relevance in the
111 microbiota's resilience to antibiotic-induced disturbances, particularly in maintaining
112 colonization resistance against invading microbes.

Results

Singly housed mice respond more heterogeneously to streptomycin than co-housed mice

In a previous study, we observed that the impact of antibiotics on the composition of the gut microbiota can vary significantly among singly housed mice²⁸. Since mice are coprophagic, co-housing has been widely used in laboratory settings as a strategy to reduce variability among untreated animals prior to experimental intervention^{20,45}. We studied the effects of this strategy during and after a dysbiotic event, to determine if the ability to share the microbiota in co-housed animals could have functional consequences, namely by influencing the colonization resistance to invading bacteria. Toward that aim, we compared the impact of antibiotics on microbiota variability, compositional dynamics, and their functional consequences in singly and co-housed mice. We independently co-housed 4 cohorts ($n=10-11$ each) of six-week-old mice for one month in one cage per cohort, and then separated them into two groups: half of the mice were kept co-housed in a single cage per cohort ($n=5$ per cage), and the remaining mice were singly housed. As soon as the mice were split into the two groups, they were continuously treated with 5 g/L of streptomycin in their drinking water for 15 days (Fig. 1a). After 15 days, the streptomycin was removed from the water, and the mice were tracked for an additional 42 days. Fecal samples were collected every 5 days during streptomycin treatment, and once per week thereafter.

16S rRNA sequencing revealed that the samples collected before antibiotic treatment mainly consisted of the two major phyla in mammalian guts: Bacteroidetes ($\approx 70\%$;

Supplementary Fig.1a) and Firmicutes ($\approx 20\%$; Supplementary Fig.1b); the other phyla accounted for $<10\%$ of the total abundance on average (Proteobacteria, Fig. 1b and Verrucomicrobia, Supplementary Fig. 1c). After 15 days of streptomycin treatment, the Bacteroidetes and Firmicutes abundances were extremely variable in singly housed mice, as compared to both co-housed in the same conditions and untreated mice (Supplementary Fig. 1a,b). The abundance of Verrucomicrobia was variable, independently of housing status (Supplementary Fig. 1c). In co-housed mice, members of the Proteobacteria phylum were always maintained and increased in abundance in most of the mice (Fig. 1b); by contrast, they decreased to very low levels in many single housed mice, with a few retaining higher levels. Six weeks after removing streptomycin (day 57), the two groups continued to differ starkly at the level of Proteobacteria presence. All co-housed mice maintained members of this phylum throughout, while only 10 of 20 singly housed mice recovered Proteobacteria (Fig. 1b). These findings highlight the increased potential for extinction in singly housed mice.

We computed the Unifrac distances between all pairs of samples within each group of each cohort at the different time points, as a measure of dissimilarity among each set of samples. As expected, during and after antibiotics, co-housed microbiotas had significantly lower mean distances than singly housed microbiotas (Fig. 1c), indicating tighter clustering. Thus, the inter-individual variation of microbiota composition (beta diversity) of streptomycin-treated mice is dependent on whether or not they are co-housed, and co-housed mice have more similar microbiotas to each other than among singly housed mice (Fig. 1c).

To quantify the size of the environmental bacterial reservoir in the two housing conditions, we calculated the number of unique operational taxonomic units (OTUs) for the co-housed mice and for each singly housed mouse. We observed that the number of unique OTUs in the cages of co-housed mice (gamma diversity) was higher during and after streptomycin treatment than in each of the singly housed mice (Fig. 1d). Furthermore, we analyzed the effect of streptomycin on prevalent OTUs for each housing condition, defined as the core OTUs present in every mouse of each group before treatment. Singly housed mice lost significantly more core OTUs than co-housed mice, both during and after treatment (Fig. 1e), confirming that the co-housed mice maintained an environmental reservoir of microbes with higher diversity. Moreover, the percentage of core OTUs increased after treatment only in the co-housed group (Supplementary Fig. 1d).

We next tested whether differences in housing would affect the response to other antibiotics as well. We carried out a controlled test for housing in a facility located on a different continent, providing a test for the generality of our results with a distinct antibiotic treatment and different starting microbiota composition (Supplementary Fig. 2a). We observed that, despite highly different microbiota composition in these animals (Supplementary Fig. 2b) and distinct mechanisms of action, ciprofloxacin and streptomycin elicited similar compositional and diversity signatures that distinguished the response of co-housed and singly housed microbiotas after antibiotic treatment. Namely, ciprofloxacin treatment resulted in lower inter-individual variation of microbiota composition in co-housed mice versus singly housed mice (Supplementary Fig. 2c) and that the number of unique OTUs in the cage of the co-housed mice was higher during and after treatment than

in each of the singly housed mice (Supplementary Fig. 2d). Overall, these data demonstrate that cohabiting mice have a more homogeneous microbiota and preserve a larger bacterial reservoir during and after antibiotic treatment than singly housed mice, which experience eradication of a subset of species that can vary between individuals.

The heterogeneous impact of antibiotics in singly housed mice leads to lower colonization resistance against E. coli

To determine whether the stochastic effects of antibiotics we observed in singly housed mice had functional implications, we sought to use colonization resistance as a property of the microbiota that might indicate a beneficial microbiota role reinforced by co-housing. Certain Proteobacteria, such as *E. coli*, colonize mammalian hosts better after antibiotic treatment, particularly streptomycin^{23,46,47}. We previously showed that a streptomycin-resistant *E. coli* strain can robustly colonize singly housed mice in the presence of streptomycin²⁸. We repeated this experiment with *E. coli* cells labeled with yellow fluorescent protein (YFP) so that they could be identified from fecal samples. We treated a cohort of mice with 5 g/L of streptomycin in drinking water (Fig. 2a). Two days after starting streptomycin treatment, the mice were gavaged with $\sim 10^8$ *E. coli* cells, and streptomycin treatment was continued after gavage. We collected samples every day after *E. coli* gavage and plated on LB agar to enumerate *E. coli* CFUs based on YFP fluorescence. The load of *E. coli* in the fecal samples were approximately 10^8 CFUs/g feces one day post-gavage and maintained or increased slightly throughout 4 days of monitoring (Fig. 2b, left).

To test the extent to which our mouse microbiotas were resistant to *E. coli* colonization, we also gavaged untreated mice with 10^8 *E. coli* cells (Fig. 2a). One day after gavage, only one of the 5 untreated mice had detectable levels of *E. coli*, and the abundance had dropped by >100-fold as compared with the inoculum; thereafter, the levels of *E. coli* were below the detection limit in all mice (Fig. 2b, right). Therefore, in the absence of antibiotics, the microbiotas of our mice are highly resistant to *E. coli* colonization, in accordance with previous reports regarding *E. coli* and *Salmonella*^{16,23,46}. Furthermore, these results validate the use of this model to determine the colonization resistance capacity of the microbiota as a measurement of the functional potential of gut microbes.

To interrogate whether there was a functional consequence of the microbiota differences between co-housed and singly housed mice after streptomycin treatment, we determined whether the microbiota from the co-housed mice had higher colonization resistance against *E. coli* than singly housed mice. We challenged all mice (co- and singly housed) from three of the initial cohorts shown in Fig. 1 with $\sim 10^8$ *E. coli* cells, after the six-week period post-streptomycin treatment (Fig. 2c). We collected fecal samples every day after *E. coli* gavage and plated on LB agar to count *E. coli* CFUs based on YFP fluorescence. Overall, co-housed mice had lower loads of *E. coli*-YFP than singly housed mice (Fig. 2d). We calculated the Area Under the Curve (AUC), for the dynamics of *E. coli*-YFP CFU/g feces during the experiment for each of the 3 cohorts tested, which allowed us to perform statistics on the *E. coli* loads kinetics between the different housing conditions. AUC values demonstrate that co-housed mice had significantly lower loads of *E. coli* throughout the experiment than singly housed mice (Fig. 2e). Interestingly, a small number of singly housed mice behaved

similarly to the co-housed group. This bimodal behavior was particularly stark in cohort 2 (dark pink and dark blue lines in Fig. 2d), in which one singly housed mouse exhibited a 1000-fold decrease in *E. coli*-YFP loads in comparison with the other singly housed mice. In this cohort, *E. coli* loads dropped steadily after gavage in all co-housed mice, decreasing by at least 2-3 orders of magnitude after 9 days, and ranged from 10^6 CFUs/g feces to undetectable levels on the last day of the experiment (dark pink lines in Fig. 2d). Only the aforementioned singly housed mouse (mouse 10) exhibited the same kinetics of decrease in *E. coli* loads as co-housed mice; all other singly housed mice maintained high levels ($>10^7$ CFUs/g feces) throughout the experiment (dark blue lines Fig. 2d). Thus, post-streptomycin treatment, maintenance of colonization resistance to *E. coli* is highly dependent on housing conditions and heterogeneous across singly housed mice.

K. michiganensis is sufficient to provide colonization resistance in antibiotic-treated mice

Although most singly housed mice were susceptible to *E. coli* colonization among the different cohorts (Fig. 2d), we were intrigued by the one mouse from the cohort 2 that behaved like the co-housed mice of the same cohort, maintaining colonization resistance and reaching 1000-fold lower *E. coli* colonization levels than its other singly housed siblings (Fig. 2d). We noticed that upon plating on LB agar, there was a higher number of non-YFP fluorescent colonies, with a different morphology from *E. coli* (Fig. 3a). These streptomycin-sensitive, non-YFP colonies were present in all co-housed samples of cohort 2. Among the singly housed mice, these colonies were only present in samples from the mouse that exhibited colonization resistance (mouse 10), and at levels as high as in co-

housed mice (Fig. 3b). Sanger sequencing of the entire 16S rRNA gene revealed that these non-YFP colonies belonged to the *Klebsiella* genus. We next analyzed the microbiota composition (Supplementary Fig. 3) present prior to *E. coli* gavage (day 57, Fig. 2c). To identify species that could confer colonization resistance against *E. coli*, we compared the microbiota sequences present in mice that provided colonization resistance against *E. coli* (i.e., all co-housed mice 1-5, and singly housed mouse 10) with the 4 singly housed mice that were susceptible to *E. coli* colonization. A metagenomic analysis using the linear discriminant analysis effect size (LEfSe)⁴⁸ method identified 2 OTUs associated with the microbiota that did not display colonization resistance (Supplementary Fig. 3b,c), and 5 OTUs associated with the microbiota that displayed colonization resistance (Supplementary Fig. 3b,d). Two of the OTUs associated with colonization resistance belonged to the *Bacteroides* genus, two to *Barnesiella*, and one to *Klebsiella* (Supplementary Fig. 3b,d). Strikingly, among these OTUs, the *Klebsiella* was the only one that was both below the detection limit in all mice that were susceptible to *E. coli*, and present in all colonization-resistant mice (with an average abundance of 4.5%, Supplementary Fig. 3d). Moreover, these *Klebsiella*-associated mice had significantly lower levels of *E. coli*-YFP when compared with the non-*Klebsiella*-associated mice from this cohort (Supplementary Fig. 3e).

In all mice from cohort 2 in which *Klebsiella* was detected on day 57 (mice 1-5 and 10), it was not possible to detect it on day 0 (prior to streptomycin treatment) by 16S sequencing (Supplementary Fig. 3a). Thus, its appearance led us to question whether *Klebsiella* is a resident of the normal microbiota of our mice but below the detection limit of 16S

sequencing, or an environmental invader of dysbiotic microbiota. To distinguish between these scenarios, we screened 28 cohorts of mice in our facility for *Klebsiella* presence over the course of one year, using a method of *Klebsiella* enrichment with selective media that has increased sensitivity of detection over 16S sequencing (see methods). We found that 25% of the cohorts tested scored positive for *Klebsiella* (Supplementary Table 1). The list of tested cohorts included cohort 3 and 4 from our housing experiments, which correspond to litter ID 23 and 27 (Supplementary Table 1), respectively. Cohort 3, but not 4, scored positive for *Klebsiella* prior to treatment (Supplementary Table 1). Interestingly, after treatment, co-housed mice but none singly housed mice from cohort 3 (and neither singly nor co-housed mice from cohort 4) had *Klebsiella* in the microbiota (Supplementary Fig. 4). These results reveal that *Klebsiella* is a low abundance member of a fraction of normal mice microbiotas, and its survival in the gut after antibiotics is very susceptible to housing conditions, whereby it often goes extinct after streptomycin treatment in singly housed mice but when present in co-housed mice is ultimately maintained in every mouse within the same cage.

The strong association between *Klebsiella* presence and colonization resistance to *E. coli* led us to hypothesize that the *Klebsiella* species could have a direct role in providing colonization resistance against *E. coli*. We performed whole-genome sequencing (WGS) on two colonies from cohort 2, one from a co-housed mouse (mouse 1) and one from the colonization-resistant singly housed mouse (mouse 10). WGS analysis revealed that this species is *Klebsiella michiganensis*, a close relative of *Klebsiella oxytoca*⁴⁹. The two isolates

were >97% identical to the NCBI genome sequence of *K. michiganensis* Kd70, a strain that lacks the pathogenic capacity of other *Klebsiella* spp.⁴⁹, and 100% identical to each other.

To test whether the *K. michiganensis* isolates were sufficient to confer colonization resistance in singly housed mice, littermates were co-housed for one month, then singly housed before treatment with streptomycin for 15 days (Fig. 3c). Four days after streptomycin treatment ended (day 19), we gavaged half of the mice with 10^8 CFUs of *K. michiganensis*, and the other half was kept as a control cohort. Four days later (day 23), all mice were gavaged with 10^8 CFUs *E. coli*-YFP (Fig. 3c). We then monitored *E. coli*-YFP loads daily for 9 days. In the mice not gavaged with *K. michiganensis*, *E. coli* CFUs remained high throughout the experiment ($\sim 10^7$ CFUs/g feces, Fig. 3d). By contrast, in all mice that were gavaged with *K. michiganensis*, while *K. michiganensis* loads remained unchanged throughout the experiment (Supplementary Fig. 5a), *E. coli*-YFP loads were significantly lower (10- to 100-fold; Fig. 3d; comparisons of the different AUC are shown in Supplementary Fig. 5b).

To test if *E. coli* load was dependent on which species arrived first in the gut, we performed an experiment in which mice were first gavaged with *E. coli*-YFP, and 4 days later were gavaged with 10^8 CFUs of either *K. michiganensis* or *E. coli*-CFP as a control (Fig. 3c). One day after *E. coli*-YFP gavage (day -3), all mice were colonized with *E. coli* at approximately 10^6 CFUs/g feces (Fig. 3e); these loads increased to approximately 10^7 CFUs/g by 4 days after gavage (day 0). As expected, in the group of mice gavaged with *E. coli*-CFP, *E. coli*-YFP loads continued to be high (10^7 - 10^8 CFUs/g feces; Fig. 3e), and *E. coli*-CFP could only

colonize at 10^3 - 10^4 CFUs/g feces since the gut was already occupied by the isogenic *E. coli*-YFP strain (Supplementary Fig. 5c). By comparison, upon introduction of *K. michiganensis*, *E. coli*-YFP loads significantly dropped continuously for the following three days, stabilizing at 10^6 CFUs/g (Fig. 3e; comparisons of the different AUC are shown in Supplementary Fig. 5d), while *K. michiganensis* loads increased to 10^9 by day 2 and then remained high (Supplementary Fig. 5c). Thus, our data indicate that *K. michiganensis* is sufficient for establishing colonization resistance to *E. coli* under streptomycin-induced dysbiosis, independent of colonization order.

K. michiganensis outcompetes E. coli through nutrient competition

To gain insight into the mechanism by which *K. michiganensis* impairs *E. coli* colonization, we investigated whether *K. michiganensis* and *E. coli* compete directly in the gut. To determine whether they occupy similar spatial locations, we imaged gut sections collected from mice that received both *E. coli* and *K. michiganensis*, staining them with 16S rRNA FISH probes that individually target Gammaproteobacteria (red) or *E. coli* specifically (green). *E. coli* cells stained with both FISH probes and therefore appeared yellow. The large, puffy, and diffuse green signal represented staining by the lectin Ulex Europaeus Agglutinin I (UEA1), which binds to mucus. Although the FISH probe specific for *E. coli* was also green, there were no bacteria-sized and shaped objects that appeared only in the green channel. *E. coli* (yellow cells) were often found in the same gut region but not in close proximity with any non-*E. coli* Gammaproteobacteria cells (red) (Fig. 4a), which we inferred to be *K. michiganensis* since *K. michiganensis* and *E. coli* were the dominant Gammaproteobacteria in these mice. In fact, all Gammaproteobacteria, including *E. coli*,

appeared to be spread out within the intestinal lumen, suggesting that they share similar niches, and thus are likely to be directly competing with each other.

To further test whether *K. michiganensis* competes directly with *E. coli*, we sought to determine whether we could detect inhibition of *E. coli* growth by *K. michiganensis in vitro*. We grew cultures of *K. michiganensis*, as well as *E. coli* expressing either CFP or YFP, separately overnight in LB. We then mixed stationary phase cultures in two combinations: *E. coli*-YFP+*E. coli*-CFP or *E. coli*-YFP+*K. michiganensis*, with OD₆₀₀=0.025 of each. These combinations were compared with individual controls of *E. coli*-YFP or *K. michiganensis* alone at initial OD₆₀₀=0.05. To create microaerobic conditions that also maximized the opportunity of cells to come into contact with each other, we grew cultures without shaking at 37 °C, as described previously⁵⁰, and measured OD₆₀₀ and YFP fluorescence for 25 h. All cultures initially grew with similar dynamics, with single and mixed cultures containing *K. michiganensis* achieving a higher density at the end of the growth curve (Fig. 4b). The combination of *E. coli*-YFP+*E. coli*-CFP grew indistinguishably from *E. coli*-YFP alone (Fig. 4b). YFP fluorescence levels in the *E. coli*-YFP+*K. michiganensis* mixtures diverged from that of the *E. coli*-YFP+*E. coli*-CFP mixtures after 7 h of growth and remained slightly lower throughout the remainder of the experiment (Fig. 4c).

Given that this decrease was consistent with a small competitive fitness advantage of *K. michiganensis* over *E. coli*, and that LB provides a rich environment for Enterobacteriaceae growth, we hypothesized that the fitness advantage of *K. michiganensis* would be greater under conditions of limited nutrients. Therefore, to create a more competitive

environment, we tested minimal media with one of several simple sugars that both species are able to consume in isolation. In the gut, Enterobacteriaceae species are likely to utilize either dietary-based sugars (fructose, glucose, arabinose and xylose)^{38,51} or mucus layer-derived simple sugars (fucose)⁵¹. Across all of these carbon sources, cultures with *K. michiganensis* had a higher growth rate and achieved a higher yield than cultures of *E. coli* only (Fig. 4d). The *E. coli*-YFP+*K. michiganensis* mixtures grew with the same dynamics as the *K. michiganensis* culture, but the YFP fluorescence levels in the *E. coli*-YFP+*K. michiganensis* mixtures were substantially decreased compared to the *E. coli*-YFP+*E. coli*-CFP mixtures (Fig. 4e). Thus, *K. michiganensis* effectively outcompetes *E. coli* in all carbon sources tested.

While these data show that *K. michiganensis* can outcompete *E. coli*, they do not distinguish between models based on metabolic competition or physical interaction. To test whether the decrease in YFP fluorescence was due to *E. coli* killing by *K. michiganensis*, we repeated the minimal media co-culturing experiments and then, at the 24-h time point, stained each sample with 10 μ M propidium iodide (PI). Live bacterial cells are usually not permeable to PI; hence, intracellular DNA-bound PI fluorescence is frequently treated as a signature of cell death. We imaged each sample and calculated the percentage of YFP- and PI-positive cells. The percentage of YFP-positive cells in all *E. coli*-YFP+*E. coli*-CFP mixtures was approximately 50%. By contrast, the percentage of YFP-positive cells in *E. coli*-YFP+*K. michiganensis* mixtures was <10%, indicating a marked inhibition of *E. coli* growth. Using the PI signal to classify dead cells, we found that <1% of all cells were dead in both mixtures (Supplementary Fig. 6a). Although we could not determine whether the dead cells

were *E. coli* or *K. michiganensis*, as dead cells could lose fluorescence, the similarly low amount of death in *E. coli*-YFP+*E. coli*-CFP and *E. coli*-YFP+*K. michiganensis* mixtures suggests that *K. michiganensis* does not kill *E. coli* cells under these conditions.

To further verify that *K. michiganensis* does not kill *E. coli in vitro*, we co-cultured *K. michiganensis* with *E. coli*-YFP in minimal medium with arabinose (the carbon source with the strongest inhibition by *K. michiganensis*) in a microfluidic device with continuous infusion of fresh medium and followed their growth by microscopy. After 12 h of time-lapse imaging, no death of *E. coli* cells was observed. Interestingly, *K. michiganensis* cells appeared to produce an extracellular matrix or capsule that resulted in large gaps between cells, which might prevent contact-mediated killing. We quantified the growth rates of *E. coli* microcolonies in the microfluidic chamber and found no significant difference between microcolonies in contact with *K. michiganensis* cells and those separated from *K. michiganensis* (Supplementary Fig. 6b). These single-cell data suggest that there is no obvious killing or contact-dependent inhibition of *E. coli* by *K. michiganensis*. Growth in a transwell system, where the two species were in separate chambers sharing the same medium (minimal medium with arabinose or fructose), further supported this conclusion: *K. michiganensis* in one chamber could still inhibit *E. coli*-YFP in the other chamber, even though the two species could not be in direct contact (Supplementary Fig. 6c). Moreover, cell-free spent medium from a *K. michiganensis* culture or from an *E. coli*-YFP+*K. michiganensis* mixed culture in minimal medium with fructose did not inhibit *E. coli*-YFP growth (Supplementary Fig. 6d). Overall, these results argue against *E. coli* killing/inhibition by either a contact-dependent mechanism or an inhibitory compound

produced by *K. michiganensis*. Instead, *K. michiganensis* cells likely have a growth advantage over *E. coli* and thereby reduce the relative abundance of *E. coli*. Therefore, we reasoned that nutritional competition is the most obvious explanation for the advantage of *K. michiganensis* over *E. coli* observed in co-cultures where the two strains compete for the same carbon source.

An E. coli-exclusive carbon source delays the colonization resistance capacity of K. michiganensis in vivo

To test if competition for nutrients could play a role in the interactions between *E. coli* and *K. michiganensis* in the gut, we hypothesized that *in vivo* colonization of *E. coli* would be facilitated by providing it with a nutritional advantage, such as a carbon source that is accessible to *E. coli* but cannot be utilized by *K. michiganensis*. Previous reports suggested that galactitol is such a carbon source⁵²; we confirmed those findings by growing monocultures of *K. michiganensis* and *E. coli* in minimal medium with galactitol in static conditions at 30 °C, the optimal temperature for *E. coli* growth with this metabolite *in vitro*. While *E. coli* grew, *K. michiganensis* showed little to no growth after >40 h, similar to a $\Delta gatZ$ *E. coli* mutant deficient in galactitol usage (Supplementary Fig. 7a).

To test whether galactitol would increase *E. coli* colonization loads in the presence of *K. michiganensis*, we treated mice with streptomycin for 15 days (Fig. 5a). Three days after treatment ended (day 18), the drinking water was supplemented with 2% galactitol. On the following day (day 19), all mice were gavaged with 10⁸ CFUs of *E. coli*-YFP and four days later (day 23) they were gavaged with 10⁸ CFUs of *K. michiganensis* (Fig. 5a). One mouse

out of 8 was found to be already colonized with *Klebsiella* upon *E. coli*-YFP gavage, as to be expected given that this mouse was from a *Klebsiella*-positive litter (litter ID 14, Supplementary Table 1). This observation provides further support for the stochastic effect of streptomycin on *K. michiganensis* abundance in singly housed mice that we observed above (Fig. 2, Supplementary Fig. 4). This mouse was removed from further consideration, since it was not possible to test the ability of *K. michiganensis* to displace *E. coli*, because the indigenous *Klebsiella* in this mouse provided *a priori* colonization resistance to *E. coli* (Supplementary Fig. 7b). One day after *E. coli*-YFP gavage, *E. coli*-YFP levels were approximately 10^7 CFU/g, and remained 10^7 - 10^8 CFU/g thereafter. Upon *K. michiganensis* gavage, the *E. coli*-YFP loads started to decrease slightly but reached 10^6 only after 6 days (Fig. 5b). These data differ significantly from our previous experiment, in which *K. michiganensis* gavage of mice drinking water without galactitol caused *E. coli*-YFP levels to drop from 10^8 to 10^6 CFUs/g feces after 3 days (Fig. 5b; comparisons of the different AUC are shown in Supplementary Fig. 7d). *K. michiganensis* levels were high throughout the experiment regardless of *E. coli*-YFP loads and the presence of galactitol (Supplementary Fig. 7c). Thus, galactitol administration staved off colonization resistance to *E. coli* for 3 days. These data show that by providing a nutritional advantage to *E. coli*, the colonization resistance capacity of *K. michiganensis* was delayed.

We reasoned that the transient effect of galactitol could be related to the presence of other microbes capable of consuming this carbon source, whose proliferation would attenuate the nutritional advantage of *E. coli* over time. To test if *E. coli* would experience a more prolonged nutritional advantage over *K. michiganensis* due to galactitol, without the

interference of other gut microbes, we compared the capacity of *K. michiganensis* to provide colonization resistance to *E. coli* with or without galactitol in the drinking water in gnotobiotic mice. As a control, we also tested the capacity of *K. michiganensis* to provide colonization resistance to a $\Delta gatZ$ *E. coli* mutant with galactitol in the drinking water. These experiments also tested if *K. michiganensis* can directly establish colonization resistance to *E. coli* in the gut in the absence of other microbiota members. Two groups of germ-free mice were supplemented with 2% galactitol in the drinking water for the duration of the experiment and compared with one group of germ-free mice with non-supplemented water (Fig. 5c). One day after starting galactitol addition (day -4), all mice were gavaged with 10^8 CFUs of *E. coli*-YFP and four days later (day 0) they were gavaged with 10^8 CFUs of *K. michiganensis* (Fig. 5c). One day after *E. coli*-YFP gavage, *E. coli*-YFP levels were approximately 10^8 CFU/g in the group of mice drinking non-supplemented water, increasing to approximately 10^9 CFU/g after 4 days. Upon *K. michiganensis* gavage, *E. coli*-YFP loads decreased immediately, dropping 1000-fold in 2 days and remaining 10^6 - 10^7 CFU/g thereafter (Fig. 5d).

By contrast, in the group of mice colonized with *E. coli*-YFP drinking galactitol-supplemented water, *E. coli*-YFP levels were already higher on day 1, ranging from 10^8 to almost 10^{10} CFUs, and stabilized at approximately 10^9 CFU/g in 4 days. Upon *K. michiganensis* gavage, *E. coli*-YFP loads decreased slightly in the first 2 days to 10^8 CFU/g, but stabilized thereafter, at significantly higher loads (10- to 100-fold) than in the group of mice drinking non-supplemented water (Fig. 5d; comparisons of the different AUC are shown in Supplementary Fig. 7f). The control group of mice colonized with $\Delta gatZ$ *E. coli*-

YFP drinking galactitol-supplemented water colonized to levels in the initial 4 days similar to *E. coli*-YFP in the same conditions (Fig. 5d), despite the inability of $\Delta gatZ$ cells to consume galactitol; this lack of a fitness change is not surprising since $\Delta gatZ$ *E. coli* is known to have higher fitness in mouse gut colonization than wild-type *E. coli*⁵³. Upon *K. michiganensis* gavage, *E. coli* $\Delta gatZ$ -YFP loads started to decrease immediately, dropping 100-fold in 2 days and remaining 10⁶-10⁷ CFU/g thereafter (Fig. 5d), similar to wild-type *E. coli*-YFP without the nutritional advantage of galactitol (Supplementary Fig. 7f). Overall, these data show that *K. michiganensis* can establish colonization resistance to *E. coli* in the gut in the absence of other microbiota members. Moreover, in the absence of other microbes, providing a nutritional advantage to *E. coli* abolishes the colonization resistance capacity of *K. michiganensis*, supporting the role of nutrient competition as the mechanistic basis of colonization resistance conferred by *K. michiganensis*.

***K. michiganensis* prolongs host survival upon *Salmonella* infection**

Our results show that upon antibiotic-induced dysbiosis, *K. michiganensis* was sufficient to provide colonization resistance to a non-pathogenic *E. coli* K-12 strain. We next tested if *K. michiganensis* would also provide colonization resistance to an enteric pathogen closely related to *E. coli*, *Salmonella enterica* serovar Typhimurium. We performed *in vitro* co-culture experiments to test whether *K. michiganensis* showed a nutrient advantage over *S. Typhimurium*-mCherry. As a control, a commensal murine *E. coli* isolated from SPF mice in our facility was used to test if other Enterobacteriaceae present in the normal murine microbiota have the same effect as *K. michiganensis*. In minimal medium with fructose or glucose, after 9-10 h of growth mCherry levels in co-cultures of *S. Typhimurium*-mCherry

with *K. michiganensis* decreased compared to *S. Typhimurium*-mCherry co-cultured with unlabeled *S. Typhimurium* or a commensal *E. coli* (Supplementary Fig. 8a). In minimal medium with arabinose or fucose, mCherry levels in co-cultures of *S. Typhimurium*-mCherry with *K. michiganensis* decreased only slightly, and at a later stage of growth (Supplementary Fig. 8a).

These results prompted us to test the colonization resistance capacity of *K. michiganensis* and a commensal *E. coli* individually against *S. Typhimurium* *in vivo*. Three groups of mice were treated with streptomycin for 15 days (Fig. 6a). Four days later, one group was gavaged with 10^8 CFUs of *K. michiganensis* and another with 10^8 CFUs of a commensal *E. coli* (day 19), and 4 days after that, all groups were gavaged with 10^4 CFUs of *S. Typhimurium* (day 23). This *S. Typhimurium* dose was chosen so that intestinal *S. Typhimurium* expansion is required, which allowed us to follow the dynamics of colonization and infection, since the mortality rate is typically high with this *S. Typhimurium* strain. In the absence of *K. michiganensis*, independent of the presence of commensal *E. coli*, on day 1 after *S. Typhimurium* gavage *S. Typhimurium* loads were $\sim 10^7$ CFUs/g feces, and reached as high as 10^8 CFUs/g feces by day 2-3 (Fig. 6b). *S. Typhimurium* loads remained high (10^6 - 10^8 CFUs/g feces) on subsequent days. By contrast, in the group of mice colonized with *K. michiganensis*, *S. Typhimurium* loads were only detectable in 7 out of 9 mice on day 1, and ranged between 10^2 - 10^5 CFUs/g feces (Fig. 6b). *S. Typhimurium* loads in all mice took 4-5 days to reach 10^8 CFUs/g feces, stabilizing in the following days around 10^7 - 10^8 CFUs/g feces (Fig. 6b; comparisons of the different AUC are shown in Supplementary Fig. 8b). *K. michiganensis* loads remained high throughout the experiment

(~10⁹ CFUs/g feces, Supplementary Fig. 8c). Overall, these results show that *K. michiganensis* but not commensal *E. coli* is able to delay gut expansion of *S. Typhimurium*, staving off full colonization by 2 days.

Importantly, the interaction between *K. michiganensis* and *S. Typhimurium* had a direct impact on the host, delaying both weight loss (Fig. 6c) and mortality (Fig. 6d). The rate of weight loss after *S. Typhimurium* infection was slightly slower in the group that was colonized with *K. michiganensis* than in the other two groups (Fig. 6c). We also checked that colonization with *K. michiganensis* did not cause alterations in body weight prior to *S. Typhimurium* infection (Supplementary Fig. 8d). Without *K. michiganensis*, in the presence or absence of commensal *E. coli* all mice died by day 6 and 7 after *S. Typhimurium* gavage, respectively, while in the presence of *K. michiganensis* mice survived until day 11. Interestingly, *K. michiganensis*-mediated colonization resistance impacted *S. Typhimurium* expansion during the period of growth before *Salmonella*-induced inflammation remodels the luminal environment¹⁶ (i.e. before day 1). The differences in the kinetics of *S. Typhimurium* expansion after day 1 in the presence and absence of *K. michiganensis* suggest that the primary effect of *K. michiganensis* is on the initial pre-inflammation expansion of *S. Typhimurium* and not on its growth during acute inflammation (Fig. 6b). Once *S. Typhimurium* has reached sufficient densities to trigger inflammation, it is able to outcompete the microbiota even in the presence of *K. michiganensis*. The observation of *K. michiganensis*' protective effect against expansion of *S. Typhimurium* in the absence of inflammation supports the idea that *K. michiganensis* engages in metabolic strategies that inhibit the growth of other Gammaproteobacteria. Moreover, this protective ability against

548 *S. Typhimurium* is not general to all other gut commensal Enterobacteriaceae, as addition
549 of a commensal *E. coli* isolate failed to protect the mice any better than the native
550 microbiota. In summary, *K. michiganensis* is able to alter the kinetics of *S. Typhimurium*
551 infection by delaying colonization and thus postponing host mortality.

Discussion

Here, we show in laboratory mice that co-housing is an important factor in establishing and maintaining colonization resistance through antibiotic-induced microbiota perturbation. Stochastic loss of key protective commensals from the gut renders singly housed mice susceptible to enteric pathogens in the absence of an environmental microbial reservoir derived from other mice. The overall benefits of co-housing are likely general across antibiotics, as singly housed animals exhibited stochastic losses of Proteobacteria during treatment with streptomycin (Fig. 1, Supplementary Fig. 1) and of Bacteroidetes during ciprofloxacin treatment (Supplementary Fig. 2). It remains unclear whether certain antibiotics are more protective of microbes that play a role in colonization resistance, motivating a broader study on how antibiotics act on a common microbiota. Effects are presumably dependent on the degree of perturbation, with higher antibiotic doses and longer treatments having a greater chance of driving extinction. In the streptomycin conditions tested, the ability to retain *K. michiganensis* was sufficient for mice to recover colonization resistance to *E. coli*. The only singly housed mouse able to retain *K. michiganensis* also maintained colonization resistance (Fig. 2 and 3, Supplementary Fig. 3), highlighting the important functional consequences of stochasticity during gut perturbations. Additionally, other microbiota functions could be similarly affected by a quantitative or relative shift in composition, as opposed to binary loss of members.

The colonization resistance capacity provided by *K. michiganensis* is likely to be grounded in nutrient competition, since a nutritional advantage provided to *E. coli* is able to delay or mitigate the aforementioned effect (Fig. 5). The importance of the commensal gut

575 microbiota in providing colonization resistance to enteric bacteria through nutrient
576 competition has been previously proposed^{54,55}; however, the identification of microbiota
577 members that are directly involved in this process is still limited to very few
578 examples^{4,19,56,57}. We showed that the capacity of *K. michiganensis* for colonization
579 resistance can also be applied to other Enterobacteriaceae, such as the human pathogen *S.*
580 *Typhimurium*. *K. michiganensis* was not only able to stave off *S. Typhimurium* expansion,
581 but, more importantly, delayed host mortality (Fig. 6). We suspect that this effect acts on
582 the pre-inflammation period of *Salmonella* infection, and further studies could focus on
583 strategies to potentiate such a mitigating effect, especially with recent reports of other non-
584 related microbiota members being able to affect other stages of *S. Typhimurium* infection⁵⁸.
585

586 In humans, widespread antibiotic treatment across the population can lead to drastic long-
587 term effects, with bacterial commensal species eradicated from the microbiota of all hosts
588 and hence unavailable for re-colonization of the microbiota. Other Western practices may
589 also be exacerbating species extinction, such as diet¹² or the use of laxatives⁴⁴. Current
590 hygiene practices in Western societies have been very efficient in preventing infections by
591 pathogenic bacteria, but have also reduced gut microbiota diversity when compared with
592 isolated groups from South America and other traditional populations⁵⁹. Despite the
593 obvious differences in mouse and human behavior that might lead to a lesser degree of
594 microbial transmission among human hosts than in mice, humans sharing the same
595 environment contain a more similar microbiota⁴⁰. Furthermore, people living lifestyles
596 with less stringent sanitation tend to share more microbes with one another than their
597 industrialized counterparts⁶⁰. Therefore, the results shown here, support the importance of

microbial sharing as means to recover from microbiota perturbation. Sanitation and hygiene practices, while beneficial for limiting spread of infectious diseases, likely also limit the spread of beneficial microbes, thus potentiating the eradication of commensal species observed in industrialized countries⁶¹.

Currently, to deal with dysbiotic microbiotas, artificial transmission by fecal microbiota transplants (FMTs) and swabbing have been successful for the treatment of *C. difficile* infections⁶² and colonization of Cesarean-section newborns⁶³, respectively. Still, donor selection for FMTs remains a critical step for sensitive recipients. Broad use of FMTs is also hampered by the difficulties of defining a healthy microbiota. Identification of key species, such as *K. michiganensis*, that are responsible for relevant microbiota functions, is of utmost importance to achieve a robust recovery from perturbations. Our study raises the hope that, for each potential pathogen, there are one or more related commensal microbes responsible for providing colonization resistance.

Our study demonstrates the importance of housing in the stochastic extinction of key protective species, providing a deeper understanding of interspecies interactions that give rise to colonization resistance. Ultimately, understanding the full repertoire of colonization resistance mechanisms will allow us to design conditions that facilitate the reacquisition of natural commensals and inspire strategies to restore microbiota composition as routine practice following antibiotic treatments¹⁹. Future therapies will likely involve personalized treatment and prophylaxis with cocktails of defined bacterial species along with their preferred prebiotics to tackle episodic infections for each patient.

Acknowledgements

The authors thank Thibault Sana, Eric Cascales, and Melanie Blokesch for helpful discussions, and João Xavier, Carles Ubeda, and Michi Taga for suggestions and for critical readings of the manuscript, and Steven Higginbottom for help with mouse experiments. The authors thank Roberto Balbontín-Soria for providing strain RB249. The authors acknowledge support from the Allen Discovery Center at Stanford on Systems Modeling of Infection (to K.M.N. and K.C.H.), and from the Portuguese national funding agency Fundação para a Ciência e Tecnologia (FCT) PTDC/BIA-MIC/4188/14 and research infrastructure ONEIDA and CONGENTO projects (LISBOA-01-0145-FEDER-016417 and LISBOA-01-0145-FEDER-022170) co-funded by FEEI - "Fundos Europeus Estruturais e de Investimento" from "Programa Operacional Regional Lisboa 2020" (to R.A.O. and K.X). K.X., R.A.O., and V.C. acknowledge FCT for individual grants IF/00831/2015, PD/BD/106000/2014, and SFRH/BPD/116806/2016, respectively. J.L.S. and K.C.H. are Chan Zuckerberg Biohub Investigators.

Methods

Ethics statement

All mouse experiments performed at Instituto Gulbenkian de Ciência (IGC) were approved by the Institutional Ethics Committee and the Portuguese National Entity (Direção Geral de Alimentação e Veterinária; Ref. number 015190), which complies with European Directive 86/609/EEC of the European Council. All mouse experiments conducted at Stanford were performed in accordance with the Administrative Panel on Laboratory Animal Care, Stanford University's IACUC.

Streptomycin treatment protocol

C57BL/6J mice bred under specific pathogen-free conditions in the animal house facility at the Instituto Gulbenkian de Ciência were used to analyze the effects of streptomycin under different housing conditions. Prior to each experiment, 6- to 8-week old male mice were first co-housed for one month in filter-top cages, and then separated into cohorts of singly housed (one per cage) or co-housed (5 per cage) mice. At this stage, mice were moved into individually ventilated cages with HEPA filters in our biosafety level 2 animal facility. Streptomycin (5 g/L) was maintained *ad libitum* in the drinking water for 15 days. Streptomycin water was replaced every 3 days. Streptomycin treatment was followed by a period of non-supplemented water, which ranged as specified according to the experiment from 4 to 42 days prior to *E. coli* or *K. michiganensis* gavage. Fecal samples were collected every 5 days during streptomycin treatment, and once per week thereafter for subsequent

microbiota composition analysis. For the assessment of *E. coli* and *K. michiganensis* loads, fecal samples were obtained daily.

Ciprofloxacin treatment protocol

Conventional Swiss-Webster mice (RFSW, Taconic) were ordered from Taconic Biosciences and allowed to equilibrate in the Stanford mouse facility for 6 weeks. To determine the effects of ciprofloxacin treatment on the gut microbiota composition of mice housed under different conditions, 6 mice were chosen at random from a group of 11 and singly housed thereafter; the remaining 5 mice were co-housed for the duration of the experiment. For antibiotic treatments, mice were orally gavaged for five days with 3 mg ciprofloxacin twice daily. Antibiotics were dissolved and administered in 200 μ L of water. Mice were then followed for a further 9 days after halting ciprofloxacin treatment. Fecal samples were collected daily, at approximately the same time of day, during and after treatment for subsequent microbiota composition analysis.

Bacterial strains and strain construction

E. coli MG1655 derivative Sm^R, $\Delta lacIZYA::frt$, $\Delta lsrK::frt$ strains ARO071-YFP ($\Delta galK::P_{lac}::yfp::amp$), ARO073-CFP ($\Delta galK::P_{lac}::cfp::amp$)²⁸, VHC015-YFP $\Delta gatZ$ ($\Delta gatZ$ Kan^R), were used. Deletion of *gatZ* from *E. coli* was introduced via bacteriophage P1-mediated transduction in ARO071²⁸ background as previously described⁶⁴, using lysates from strain JW2082⁶⁵. *K. michiganensis* (isolated through plating on LB agar from a mouse fecal sample during this study), mouse commensal *E. coli* (isolated through plating on LB agar from a mouse fecal sample during this study), and wild-type *Salmonella enterica*

serovar Typhimurium strain ATCC 14028 transformed with pMP7605-Gent^R-mCherry⁶⁶ (RB249) were also used in this study.

Colonization resistance experiment

To assess the colonization resistance capacity of co-housed versus singly housed mice, 42 days after stopping streptomycin treatment, mice were gavaged with 100 μ L of PBS containing 10^8 colony-forming units (CFUs) of AR0071 (*E. coli* Δ lrrK YFP). Bacteria were prepared for gavage via growth to late stationary phase followed by sub-culturing to an OD₆₀₀~2, corresponding to approximately 10^9 CFUs/mL. Bacteria were pelleted and re-suspended in sterile PBS at this same concentration. Following gavage, fecal samples were collected from each mouse daily for 9 days. Fecal material was weighed, homogenized in 1 mL of sterile PBS, diluted, and plated on LB agar to determine colonization levels. Fluorescently labeled colonies were counted on a stereoscope (SteREO Lumar, Carl Zeiss) to calculate the number of *E. coli* CFUs/g feces.

To determine the capacity of *K. michiganensis* to displace or provide colonization resistance against *E. coli*, after 15 days of streptomycin treatment, singly housed mice were given either non-supplemented water for the remainder of the experiment, or non-supplemented water for 3 days and then water supplemented with 2% galactitol. Galactitol water was replaced every 2 days and prepared by dissolving galactitol powder in hot water and then allowing it to cool down before being given to mice. Four days after stopping antibiotic treatment, mice were gavaged with 100 μ L of PBS containing 10^8 CFUs of either *K. michiganensis* or *E. coli*-YFP, and four days after that either not gavaged again or gavaged

703 with 100 μ L of PBS containing 10^8 CFUs of *K. michiganensis*, *E. coli*-YFP, or *E. coli*-CFP.
704 Following the first gavage, fecal samples were collected from each mouse daily for 13 days.
705 Fecal material was weighed, homogenized in 1 mL of sterile PBS, diluted, and plated on LB
706 agar supplemented with streptomycin (100 μ g/mL) to determine colonization levels of *E.*
707 *coli* and on LB agar to determine *K. michiganensis* loads. The ability of *K. michiganensis* to
708 displace *E. coli* was also tested in ex-germ-free mice in which the same protocol was used
709 with and without water supplementation with 2% galactitol. Conditions tested: *E. coli*-YFP
710 colonization challenged with *K. michiganensis*; *E. coli*-YFP colonization challenged with *K.*
711 *michiganensis*, with galactitol added to the drinking water; *E. coli*-YFP Δ *gatZ* (VHC015)
712 colonization challenged with *K. michiganensis* with galactitol added to the drinking water.
713 *E. coli*-YFP Δ *gatZ* is a strain impaired in galactitol consumption.
714
715 To determine the capacity of *K. michiganensis* or a mouse commensal *E. coli* to provide
716 colonization resistance to *S. Typhimurium*, after 15 days of streptomycin treatment, singly
717 housed mice were given non-supplemented water for the remainder of the experiment.
718 Four days after stopping antibiotic treatment, one group of mice was gavaged with 100 μ L
719 of PBS containing 10^8 CFUs of *K. michiganensis*, another group was gavaged with 100 μ L of
720 PBS containing 10^8 CFUs of commensal *E. coli*, and a final group was not gavaged. Four days
721 after the first gavage, all groups were gavaged with 100 μ L of PBS containing 10^4 CFUs of *S.*
722 *Typhimurium*. Following the first gavage, fecal samples were collected from each mouse
723 daily for 13 days. Fecal material was weighed, homogenized in 1 mL of sterile PBS, diluted,
724 and plated on LB agar supplemented with gentamycin (30 μ g/mL) to determine
725 colonization levels of *S. Typhimurium* and on LB agar to determine *K. michiganensis* or

commensal *E. coli* loads. According to the approved ethical protocol for animal experimentation, mice that presented extreme weight loss (20% of initial weight) or were lethargic/moribund due to *S. Typhimurium* infection were humanely sacrificed.

***Klebsiella* detection**

A fecal sample from 1 mouse per cohort was collected and homogenized in 1 mL of sterile PBS. *Klebsiella* spp. are known to degrade complex plant cell wall polysaccharides, such as cellobiose, through carbohydrate-active enzymes⁶⁷. Therefore, five milliliters of minimal medium with 0.4% cellobiose was inoculated with 100 µL of fecal suspension in glass tubes, and grown overnight at 37 °C with shaking. The overnight culture was serially diluted and plated on LB agar. All colonies with similar morphology to *Klebsiella* were streaked in Brilliance ESBL Agar (OX; Oxoid, Basingstoke, United Kingdom), and positive clones for *Klebsiella* species (according to the manufacturer's instructions) were sent for Sanger sequencing of the 16S rRNA gene, using the primers 27f (5'-GAGAGTTTGATCCTGGCTCAG-3') and 1495r (5'-CTACGGCTACCTTGTACGA-3')⁶⁸ and the following reaction: 95 °C for 1 min, followed by 30 cycles of 15 s denaturation at 95 °C, 15 s at 57 °C, and 45 s at 72 °C, after which a final extension at 72 °C was performed for 10 min.

Whole genome sequencing

One *Klebsiella* clone was isolated from the feces of mice 1 and another mouse 10 (cohort 2) and grown in LB at 37 °C with agitation for subsequent DNA isolation using a previously described protocol⁶⁹. A DNA library was constructed and sequenced by the IGC Genomics facility. Paired-end sequencing of each sample was performed on an Illumina MiSeq

Benchtop Sequencer (Illumina, San Diego, CA), which produced datasets of 250-bp read pairs. *K. michiganensis* genomes will be deposited in a public database prior publication.

Preparation of tissue sections for imaging

Mice were euthanized with CO₂ and death was confirmed by cervical dislocation. After sacrifice, sections of the intestinal tract (colon) were fixed using paraformaldehyde. They were then embedded, sectioned, and stained as previously described⁷⁰. Briefly, two sections per mouse were fixed in 2% paraformaldehyde in phosphate buffer for 16-18 h, washed in 70% ethanol, and then paraffin-embedded. Samples were sectioned into 4 µm-thick sections for staining with DAPI, fluorescence in situ hybridization probes targeting Gammaproteobacteria (Gam42A: 5'-GCCTTCCCACATCGTTT-3') and *E. coli* (Eco1167: 5'-GCATAAGCGTCGCTGCCG-3')⁷¹, and lectins targeting mucin carbohydrates (Vector Laboratories, Burlingame, CA). Fluorescence in situ hybridization was performed as previously described⁷⁰. Sections of the distal colon were imaged on a Zeiss LSM 880 confocal microscope equipped with an Airyscan super-resolution module. Airyscan images were processed using Zen Blue and FIJI.

16S rRNA sequencing

For streptomycin-treatment experiments, fecal samples were stored at -80 °C and DNA extraction was performed as previously described²⁸. In brief, DNA was extracted using a combination of the QIAamp Fast DNA Stool Mini Kit (Qiagen) following the manufacturer's instructions, mechanically disrupted with a tissue blender, and eluted to a final volume of 100 µL in ATE buffer. For each sample, the 16S rRNA gene was amplified using the Earth

Microbiome Project-recommended 515F/806R primer pairs (V3-V4 regions) under the following PCR cycling conditions: 94 °C for 3 min, 35 cycles of 94 °C for 60 s, 50 °C for 60 s, and 72 °C for 105 s, with an extension step at 72 °C for 10 min^{72,73}. After library prep, 2x250-bp sequencing was performed at the IGC Genomics Unit using an Illumina MiSeq Benchtop Sequencer.

For ciprofloxacin-treatment experiments, fecal samples were frozen and stored at -80 °C prior to DNA extraction. DNA was extracted from whole fecal pellets with the PowerSoil-htp kit (MO BIO, San Diego, CA). DNA extracted from fecal samples was used to generate 16S rRNA amplicons using the Earth Microbiome Project-recommended 515F/806R primer pairs. PCR products were cleaned, quantified, and pooled using the UltraClean 96 PCR Cleanup kit (MO BIO, San Diego, CA) and Quant-It dsDNA High Sensitivity Assay kit (Invitrogen, Carlsbad CA). Samples were pooled and sent to the Mayo Clinic's Molecular Biology Core (Rochester, MN) for 2x300-bp MiSeq (Illumina, San Diego, CA) library prep and sequencing.

Sequencing data analyses

Mothur v. 1.32.1 was used to process sequences as previously described⁷⁴, with some modifications. Sequences were converted to FASTA format. Sequences shorter than 220 bp containing homopolymers longer than 8 bp or undetermined bases, with no exact match with the forward and reverse primers and barcodes, that did not complement each other, or that did not align with the appropriate 16S rRNA variable region were not included in the analysis. A quality score above 30 (range is from 0 to 40, with 0 representing an

ambiguous base), was used to process sequences, which were trimmed using a sliding-window technique over a 50-base window. Sequences were trimmed from the 3' end until the quality score criterion was met, and merged after that. A range between 20,000 and 50,000 sequences was obtained per sample. 16S rRNA gene sequences were aligned using SILVA template reference alignment⁷⁵. *ChimeraSlayer*⁷⁶ was used to remove potential chimeric sequences. Sequences with distance-based similarity above 97% were joined into the same operational taxonomic unit (OTU) using the average-neighbor algorithm. All samples were rarefied to the same number of sequences (10,000) for diversity analyses. OTU-based microbial gamma-diversity was estimated by calculating the total number of unique OTUs in each cage at each time point. A Bayesian classifier algorithm with a 60% bootstrap cutoff was used for each sequence⁷⁷, which was assigned to the genus level where possible or the closest genus-level classification otherwise and preceded by “unclassified”. The Clearcut algorithm⁷⁸ was used to infer a phylogenetic tree based on the 16S rRNA sequence alignment, which was used to calculate unweighted and weighted UniFrac distances between each pair of samples.

To identify OTUs with differential abundances in the microbiota of mice with and without colonization resistance to *E. coli*, we utilized the linear discriminant analysis (LDA) effect size (LEfSe) method⁴⁸. LEfSe uses the Kruskal-Wallis rank-sum test on a normalized relative abundance matrix to detect significantly different OTU features and estimates the effect size of each feature via LDA. Only features with LDA scores above 2 and $\alpha < 0.05$ were considered different between the groups of mice.

To assess the loss of important OTUs during and after antibiotic treatment in mice under different housing conditions, we identified prevalent OTUs in untreated conditions as those that were present in every mouse of each group in each cohort tested (core OTUs), and then followed the dynamics of maintenance and loss of those OTUs in the same mice both during (day 15) and after (day 57) antibiotic treatment.

Custom MATLAB (MathWorks, Natick, MA) scripts were used to analyze taxa distributions across microbiota time courses.

Competition of *E. coli* and *K. michiganensis* in liquid cultures

Single colonies of *E. coli*-YFP, *E. coli*-CFP, and *K. michiganensis* were used to inoculate separate 3-5 mL cultures in LB medium in glass tubes, and grown overnight at 37 °C with shaking to an OD₆₀₀~5-5.5. The overnight cultures were diluted into 96-well plates such that the total culture inoculation OD₆₀₀ was 0.05; i.e., single cultures of *E. coli*-YFP, *E. coli*-CFP, *K. michiganensis*, or *S. Typhimurium*-mCherry were tested with an initial OD₆₀₀ of 0.05, while co-cultures of *E. coli*-YFP+*E. coli*-CFP, *E. coli*-YFP+*K. michiganensis*, *S. Typhimurium*-mCherry+*K. michiganensis*, or *S. Typhimurium*-mCherry+*E. coli*-CFP were tested with an initial OD₆₀₀ of 0.025 of each strain. Single and co-cultures were grown in either LB medium or M9 minimal medium with a single carbon source at 0.25% (w/v). Carbon sources tested were glucose, fructose, xylose, arabinose, fucose, or galactitol, as specified.

For the contact-dependent inhibition/killing assay, an overnight culture of *E. coli*-YFP was diluted into 24-well plates, and an overnight culture of *E. coli*-CFP or *K. michiganensis* was

diluted into upper chambers of transwells (0.4- μ m Millicell, Millipore) such that each chamber had an inoculation OD₆₀₀ of 0.025. Cultures were inoculated in M9 minimal medium with arabinose or fructose at 0.25% (w/v). Additionally, an overnight culture of *E. coli*-YFP was diluted into wells of a 96-well plate in M9 minimal medium with fructose at 0.25% (w/v) with or without supplementation of 20% cell-free spent medium. Cell-free spent media were obtained using 0.2- μ m Acrodisc syringe filters (Pall Corporation) from overnight cultures of *K. michiganensis* or *E. coli*-YFP+*K. michiganensis* grown in minimal medium with fructose at 0.25% (w/v).

All growth curves were performed in a Thermo-Shaker Grant-bio plate reader (Thermo Fisher Scientific) without shaking at 37 °C, except for galactitol experiments, which were performed at 30 °C. Each co-culture condition was tested in six replicates across two independent experiments, and each transwell and cell-free spent medium condition was tested in triplicate. OD₆₀₀, YFP fluorescence (excitation 485 nm, emission filter 535 nm; Victor3 (PerkinElmer)), and mCherry fluorescence (excitation 520 nm, emission filter 580-640 nm; Glomax Explorer (Promega)) were measured at various time points during growth, with 5 s of orbital shaking before each reading.

Single-cell imaging with PI staining

Mixed cultures of *E. coli*-YFP+*E. coli*-CFP and *E. coli*-YFP+*K. michiganensis* were grown statically for 24 h in various carbon sources. The final cultures were mixed with 10 μ M of propidium iodide and incubated at room temperature for 5 min. Samples were imaged on 1% agarose pads with a Nikon Ti-E inverted microscope (Nikon Instruments) using a 100X

(NA 1.40) oil immersion objective and a Zyla 5.5 sCMOS camera (Andor Technology). Images were acquired using μ Manager v. 1.4 (<http://www.micro-manager.org>).

Microfluidics

Microfluidic single-cell experiments were performed in ONIX B04A microfluidic chips (CellASIC). Since the microfluidic chamber selects cells by their size, the slightly larger size of *K. michiganensis* cells meant that they were less likely to get into the microfluidic viewing chamber. To address this disparity, we introduced a 10:1 ratio of *K. michiganensis* and *E. coli* cells. Prior to loading cells into the chamber, the cells were well mixed by pressurizing wells #6 and #8 alternately for 10 cycles. Phase-contrast and epifluorescence images were acquired on a Nikon Ti-E with a 100X (NA 1.4) objective and Andor Neo 5.5 sCMOS Camera. Cells were maintained at 37 °C during imaging using an active-control environmental chamber (Haison Technology).

Growth rate analyses of microcolonies in microfluidic experiments

When introduced into the microfluidic chamber, the vast majority of cells were initially not touching any other cells. During growth, each individual cell formed a microcolony, and the edges of microcolonies gradually merged. We visually identified *E. coli* microcolonies that either stayed away from any *K. michiganensis* microcolonies during $t = 2 - 4$ h, or those with at least 50% of the periphery directly touching *K. michiganensis* cells during the same period. The $t = 2 - 4$ h time interval was chosen because cells grew exponentially during that period, and also contained enough microcolonies in each group (isolated vs. *K. michiganensis*-proximal) for statistical analysis. Microcolony areas at each time point were

calculated by identifying the YFP+ regions in the image. Growth rates were obtained by linear fitting of the slope of natural logarithm of microcolony area over time.

Quantification and statistical analyses

To determine statistically significant differences in the relative abundances of taxa and OTUs between the groups of mice, the non-parametric Wilcoxon test was applied using the `wilcox.test` function in the 'stats' R package. Taxa and OTUs with fewer than 100 counts in both groups were not included in the analysis. To adjust for multiple hypothesis testing, we used the Benjamini-Hochberg FDR approach⁷⁹ with the `fdr.R` package. Results with $p < 0.05$ and $q < 0.1$ were considered statistically significant. To assess significant differences in kinetic curves, we calculated the Area Under the Curve (AUC) for each sample using *Graphpad Prism* v. 8, after which the AUC values for each group were evaluated using the Mann-Whitney test or Kruskal-Wallis test with Dunn's correction test for multiple comparisons. Survival assays were analyzed using the Log-Rank (Mantel-Cox) test. To compare UniFrac distances between time points during and after streptomycin or ciprofloxacin treatment, a Mann-Whitney test was used. Graphical representations were obtained using *Graphpad Prism* v. 8, MATLAB 2015b, and *RStudio* v. 3.3.3.

References

1. Flint, H. J., Scott, K. P., Louis, P. & Duncan, S. H. The role of the gut microbiota in nutrition and health. *Nat. Rev. Gastroenterol. Hepatol.* **9**, 577–589 (2012).
2. Hooper, L. V., Littman, D. R. & Macpherson, A. J. Interactions Between the Microbiota and the Immune System. *Science* **336**, 1268–1273 (2012).
3. Rakoff-Nahoum, S., Paglino, J., Eslami-Varzaneh, F., Edberg, S. & Medzhitov, R. Recognition of commensal microflora by toll-like receptors is required for intestinal homeostasis. *Cell* **118**, 229–241 (2004).
4. Ubeda, C., Djukovic, A. & Isaac, S. Roles of the intestinal microbiota in pathogen protection. *Clin. Transl. Immunol.* **6**, e128 (2017).
5. Baumler, A. J. & Sperandio, V. Interactions between the microbiota and pathogenic bacteria in the gut. *Nature* **535**, 85–93 (2016).
6. Pamer, E. G. Resurrecting the intestinal microbiota to combat antibiotic-resistant pathogens. *Science* **352**, 535–538 (2016).
7. Wopereis, H., Oozeer, R., Knipping, K., Belzer, C. & Knol, J. The first thousand days - intestinal microbiology of early life: establishing a symbiosis. *Pediatr. Allergy Immunol.* **25**, 428–438 (2014).
8. Caporaso, J. G. *et al.* Moving pictures of the human microbiome. *Genome Biol.* **12**, R50 (2011).
9. Cho, I. *et al.* Antibiotics in early life alter the murine colonic microbiome and adiposity. *Nature* **488**, 621–626 (2012).
10. Fragiadakis, G. K. *et al.* Links between environment, diet, and the hunter-gatherer

- microbiome. *Gut Microbes* 1–12 (2018). doi:10.1080/19490976.2018.1494103
11. Goodrich, J. K. *et al.* Human Genetics Shape the Gut Microbiome. *Cell* **159**, 789–799 (2014).
12. Blaser, M. J. *Missing Microbes: How the Overuse of Antibiotics Is Fueling Our Modern Plagues.* Henry Holt and Company LLC, New York **35**, (Macmillan, 2014).
13. Sekirov, I. *et al.* Antibiotic-induced perturbations of the intestinal microbiota alter host susceptibility to enteric infection. *Infect. Immun.* **76**, 4726–4736 (2008).
14. Buffie, C. G. *et al.* Profound alterations of intestinal microbiota following a single dose of clindamycin results in sustained susceptibility to *Clostridium difficile*-induced colitis. *Infect. Immun.* **80**, 62–73 (2012).
15. Ubeda, C. *et al.* Vancomycin-resistant *Enterococcus* domination of intestinal microbiota is enabled by antibiotic treatment in mice and precedes bloodstream invasion in humans. *J. Clin. Invest.* **120**, 4332–4341 (2010).
16. Stecher, B. *et al.* *Salmonella enterica* serovar typhimurium exploits inflammation to compete with the intestinal microbiota. *PLoS Biol.* **5**, 2177–2189 (2007).
17. Clasener, H. A., Vollaard, E. J. & van Saene, H. K. Long-term prophylaxis of infection by selective decontamination in leukopenia and in mechanical ventilation. *Rev. Infect. Dis.* **9**, 295–328
18. van der Leur, J. J. J. P. M., Thunnissen, P. L. M., Clasener, H. A. L., Muller, N. F. & Dofferhoff, A. S. M. Effects of Imipenem, Cefotaxime and Cotrimoxazole on Aerobic Microbial Colonization of the Digestive Tract. *Scand. J. Infect. Dis.* **25**, 473–478 (1993).
19. Keith, J. W. & Pamer, E. G. Enlisting commensal microbes to resist antibiotic-resistant

950 pathogens. *J. Exp. Med.* **216**, 10–19 (2019).

951 20. Velazquez, E. M. *et al.* Endogenous Enterobacteriaceae underlie variation in
 952 susceptibility to Salmonella infection. *Nat. Microbiol.* **4**, 1057–1064 (2019).

953 21. Pereira, F. C. & Berry, D. Microbial nutrient niches in the gut. *Environ. Microbiol.* **19**,
 954 1366–1378 (2017).

955 22. Apperloo-Renkema, H. Z., Van der Waaij, B. D. & Van der Waaij, D. Determination of
 956 colonization resistance of the digestive tract by biotyping of Enterobacteriaceae.
 957 *Epidemiol. Infect.* **105**, 355–361 (1990).

958 23. Spees, A. M. *et al.* Streptomycin-induced inflammation enhances Escherichia coli gut
 959 colonization through nitrate respiration. *MBio* **4**, (2013).

960 24. Winter, S. E. *et al.* Host-derived nitrate boosts growth of E. coli in the inflamed gut.
 961 *Science* **339**, 708–711 (2013).

962 25. Jacobson, A. *et al.* A Gut Commensal-Produced Metabolite Mediates Colonization
 963 Resistance to Salmonella Infection. *Cell Host Microbe* **24**, 296-307.e7 (2018).

964 26. Buffie, C. G. *et al.* Precision microbiome reconstitution restores bile acid mediated
 965 resistance to Clostridium difficile. *Nature* **517**, 205–8 (2014).

966 27. Hsiao, A. *et al.* Members of the human gut microbiota involved in recovery from
 967 Vibrio cholerae infection. *Nature* **515**, 423–6 (2014).

968 28. Thompson, J. A., Oliveira, R. A., Djukovic, A., Ubeda, C. & Xavier, K. B. Manipulation of
 969 the Quorum Sensing Signal AI-2 Affects the Antibiotic-Treated Gut Microbiota. *Cell*
 970 *Rep.* **10**, 1861–1871 (2015).

971 29. Cherrington, C. A., Hinton, M. & Chopra, I. Effect of short-chain organic acids on
 972 macromolecular synthesis in Escherichia coli. *J. Appl. Bacteriol.* **68**, 69–74 (1990).

- 973 30. Fay, J. P. & Farias, R. N. The inhibitory action of fatty acids on the growth of
974 *Escherichia coli*. *J. Gen. Microbiol.* **91**, 233–240 (1975).
- 975 31. Kirkpatrick, C. *et al.* Acetate and formate stress: opposite responses in the proteome
976 of *Escherichia coli*. *J. Bacteriol.* **183**, 6466–6477 (2001).
- 977 32. Wilson, K. H. Efficiency of various bile salt preparations for stimulation of
978 *Clostridium difficile* spore germination. *J. Clin. Microbiol.* **18**, 1017–1019 (1983).
- 979 33. Sassone-Corsi, M. *et al.* Microcins mediate competition among Enterobacteriaceae in
980 the inflamed gut. *Nature* **540**, 280–283 (2016).
- 981 34. Sana, T. G. *et al.* Salmonella Typhimurium utilizes a T6SS-mediated antibacterial
982 weapon to establish in the host gut. *Proc. Natl. Acad. Sci. U. S. A.* **113**, E5044-51
983 (2016).
- 984 35. Wexler, A. G. *et al.* Human symbionts inject and neutralize antibacterial toxins to
985 persist in the gut. *Proc. Natl. Acad. Sci.* **113**, 3639–3644 (2016).
- 986 36. Rabiou, B. A. & Gibson, G. R. Carbohydrates: a limit on bacterial diversity within the
987 colon. *Biol. Rev. Camb. Philos. Soc.* **77**, 443–453 (2002).
- 988 37. Crombach, A. & Hogeweg, P. Evolution of resource cycling in ecosystems and
989 individuals. *BMC Evol. Biol.* **9**, 122 (2009).
- 990 38. Conway, T. & Cohen, P. S. Commensal and Pathogenic *Escherichia coli* Metabolism in
991 the Gut. 1–15 (2015). doi:10.1128/microbiolspec.MBP-0006-2014.Correspondence
- 992 39. Fabich, A. J. *et al.* Comparison of carbon nutrition for pathogenic and commensal
993 *Escherichia coli* strains in the mouse intestine. *Infect. Immun.* **76**, 1143–1152 (2008).
- 994 40. Taur, Y. *et al.* Reconstitution of the gut microbiota of antibiotic-treated patients by
995 autologous fecal microbiota transplant. *Sci. Transl. Med.* **10**, (2018).

- 996 41. Schulfer, A. F. *et al.* The impact of early-life sub-therapeutic antibiotic treatment
997 (STAT) on excessive weight is robust despite transfer of intestinal microbes. *ISME J.*
998 (2019). doi:10.1038/s41396-019-0349-4
- 999 42. Song, S. J. *et al.* Cohabiting family members share microbiota with one another and
1000 with their dogs. *Elife* **2**, e00458 (2013).
- 1001 43. Reese, A. T. *et al.* Antibiotic-induced changes in the microbiota disrupt redox
1002 dynamics in the gut. *Elife* **7**, (2018).
- 1003 44. Tropini, C. *et al.* Transient Osmotic Perturbation Causes Long-Term Alteration to the
1004 Gut Microbiota. *Cell* **173**, 1742-1754.e17 (2018).
- 1005 45. Franklin, C. L. & Ericsson, A. C. Microbiota and reproducibility of rodent models. *Lab*
1006 *Anim. (NY)*. **46**, 114–122 (2017).
- 1007 46. Barthel, M. *et al.* Pretreatment of mice with streptomycin provides a *Salmonella*
1008 enterica serovar Typhimurium colitis model that allows analysis of both pathogen
1009 and host. *Infect. Immun.* **71**, 2839–2858 (2003).
- 1010 47. Leatham, M. P. *et al.* Precolonized human commensal *Escherichia coli* strains serve as
1011 a barrier to *E. coli* O157:H7 growth in the streptomycin-treated mouse intestine.
1012 *Infect. Immun.* **77**, 2876–2886 (2009).
- 1013 48. Segata, N. *et al.* Metagenomic biomarker discovery and explanation. *Genome Biol.* **12**,
1014 R60 (2011).
- 1015 49. Dantur, K. I. *et al.* The Endophytic Strain *Klebsiella michiganensis* Kd70 Lacks
1016 Pathogenic Island-Like Regions in Its Genome and Is Incapable of Infecting the
1017 Urinary Tract in Mice. *Front. Microbiol.* **9**, 1548 (2018).
- 1018 50. Chang, D.-E. *et al.* Carbon nutrition of *Escherichia coli* in the mouse intestine. *Proc.*

1019 *Natl. Acad. Sci. U. S. A.* **101**, 7427–7432 (2004).

1020 51. Flint, H. J., Scott, K. P., Duncan, S. H., Louis, P. & Forano, E. Microbial degradation of
 1021 complex carbohydrates in the gut. *Gut Microbes* **3**, 289–306 (2012).

1022 52. Saha, R., Farrance, C. E., Verghese, B., Hong, S. & Donofrio, R. S. *Klebsiella*
 1023 *michiganensis* sp. nov., a new bacterium isolated from a tooth brush holder. *Curr.*
 1024 *Microbiol.* **66**, 72–78 (2013).

1025 53. Barroso-Batista, J. *et al.* The first steps of adaptation of *Escherichia coli* to the gut are
 1026 dominated by soft sweeps. *PLoS Genet.* **10**, e1004182 (2014).

1027 54. Maltby, R., Leatham-Jensen, M. P., Gibson, T., Cohen, P. S. & Conway, T. Nutritional
 1028 basis for colonization resistance by human commensal *Escherichia coli* strains HS
 1029 and Nissle 1917 against *E. coli* O157:H7 in the mouse intestine. *PLoS One* **8**, e53957
 1030 (2013).

1031 55. Stecher, B. *et al.* Like will to like: abundances of closely related species can predict
 1032 susceptibility to intestinal colonization by pathogenic and commensal bacteria. *PLoS*
 1033 *Pathog.* **6**, e1000711 (2010).

1034 56. Kamada, N. *et al.* Regulated virulence controls the ability of a pathogen to compete
 1035 with the gut microbiota. *Science* **336**, 1325–1329 (2012).

1036 57. Deriu, E. *et al.* Probiotic bacteria reduce *salmonella typhimurium* intestinal
 1037 colonization by competing for iron. *Cell Host Microbe* **14**, 26–37 (2013).

1038 58. Herp, S. *et al.* *Mucispirillum schaedleri* Antagonizes *Salmonella* Virulence to Protect
 1039 Mice against Colitis. *Cell Host Microbe* **25**, 681-694.e8 (2019).

1040 59. Clemente, J. C. *et al.* The microbiome of uncontacted Amerindians. *Sci. Adv.* **1**,
 1041 e1500183 (2015).

60. Martinez, I. *et al.* The gut microbiota of rural papua new guineans: composition, diversity patterns, and ecological processes. *Cell Rep.* **11**, 527–538 (2015).
61. Sonnenburg, E. D. & Sonnenburg, J. L. The ancestral and industrialized gut microbiota and implications for human health. *Nat. Rev. Microbiol.* **17**, 383–390 (2019).
62. van Nood, E. *et al.* Duodenal infusion of donor feces for recurrent *Clostridium difficile*. *N. Engl. J. Med.* **368**, 407–415 (2013).
63. Dominguez-Bello, M. G. *et al.* Partial restoration of the microbiota of cesarean-born infants via vaginal microbial transfer. *Nat. Med.* **22**, 250–253 (2016).
64. Malke, H. T. J. Silhavy, M. L. Berman and L. W. Enquist (Editors), Experiments with Gene Fusions. 303 S., 32 Abb., 11 Tab. Cold Spring Harbor 1984. Cold Spring Harbor Laboratory. \$ 48.00. ISBN: 0-87969-163-8. *J. Basic Microbiol.* **25**, 350 (1985).
65. Baba, T. *et al.* Construction of *Escherichia coli* K-12 in-frame, single-gene knockout mutants: the Keio collection. *Mol. Syst. Biol.* **2**, 2006.0008 (2006).
66. Shyntum, D. Y. *et al.* *Pantoea ananatis* Utilizes a Type VI Secretion System for Pathogenesis and Bacterial Competition. *Mol. Plant. Microbe. Interact.* **28**, 420–431 (2015).
67. Yu, Z. *et al.* Complete genome sequence of N₂-fixing model strain *Klebsiella* sp. nov. M5a1, which produces plant cell wall-degrading enzymes and siderophores. *Biotechnol. reports (Amsterdam, Netherlands)* **17**, 6–9 (2018).
68. Bianciotto, V. *et al.* An obligately endosymbiotic mycorrhizal fungus itself harbors obligately intracellular bacteria. *Appl. Environ. Microbiol.* **62**, 3005–3010 (1996).
69. Wilson, K. Preparation of genomic DNA from bacteria. *Curr. Protoc. Mol. Biol.* **Chapter 2**, Unit 2.4 (2001).

70. Earle, K. A. *et al.* Quantitative Imaging of Gut Microbiota Spatial Organization. *Cell Host Microbe* **18**, 478–488 (2015).
71. Dejea, C. M. *et al.* Microbiota organization is a distinct feature of proximal colorectal cancers. *Proc. Natl. Acad. Sci. U. S. A.* **111**, 18321–18326 (2014).
72. Caporaso, J. G. *et al.* Ultra-high-throughput microbial community analysis on the Illumina HiSeq and MiSeq platforms. *ISME J.* **6**, 1621–1624 (2012).
73. Caporaso, J. G. *et al.* Global patterns of 16S rRNA diversity at a depth of millions of sequences per sample. *Proc. Natl. Acad. Sci. U. S. A.* **108 Suppl**, 4516–4522 (2011).
74. Kozich, J. J., Westcott, S. L., Baxter, N. T., Highlander, S. K. & Schloss, P. D. Development of a dual-index sequencing strategy and curation pipeline for analyzing amplicon sequence data on the MiSeq Illumina sequencing platform. *Appl. Environ. Microbiol.* **79**, 5112–5120 (2013).
75. Pruesse, E. *et al.* SILVA: a comprehensive online resource for quality checked and aligned ribosomal RNA sequence data compatible with ARB. *Nucleic Acids Res.* **35**, 7188–7196 (2007).
76. Haas, B. J. *et al.* Chimeric 16S rRNA sequence formation and detection in Sanger and 454-pyrosequenced PCR amplicons. *Genome Res.* **21**, 494–504 (2011).
77. Wang, Q., Garrity, G. M., Tiedje, J. M. & Cole, J. R. Naive Bayesian classifier for rapid assignment of rRNA sequences into the new bacterial taxonomy. *Appl. Environ. Microbiol.* **73**, 5261–5267 (2007).
78. Sheneman, L., Evans, J. & Foster, J. A. Clearcut: a fast implementation of relaxed neighbor joining. *Bioinformatics* **22**, 2823–2824 (2006).
79. Benjamini, Y. & Hochberg, Y. Controlling the False Discovery Rate: A Practical and

- 1088 Powerful Approach to Multiple Testing. *Journal of the Royal Statistical Society. Series*
1089 *B (Methodological)* **57**, 289–300 (1995).
1090

Figures and Figure Legends

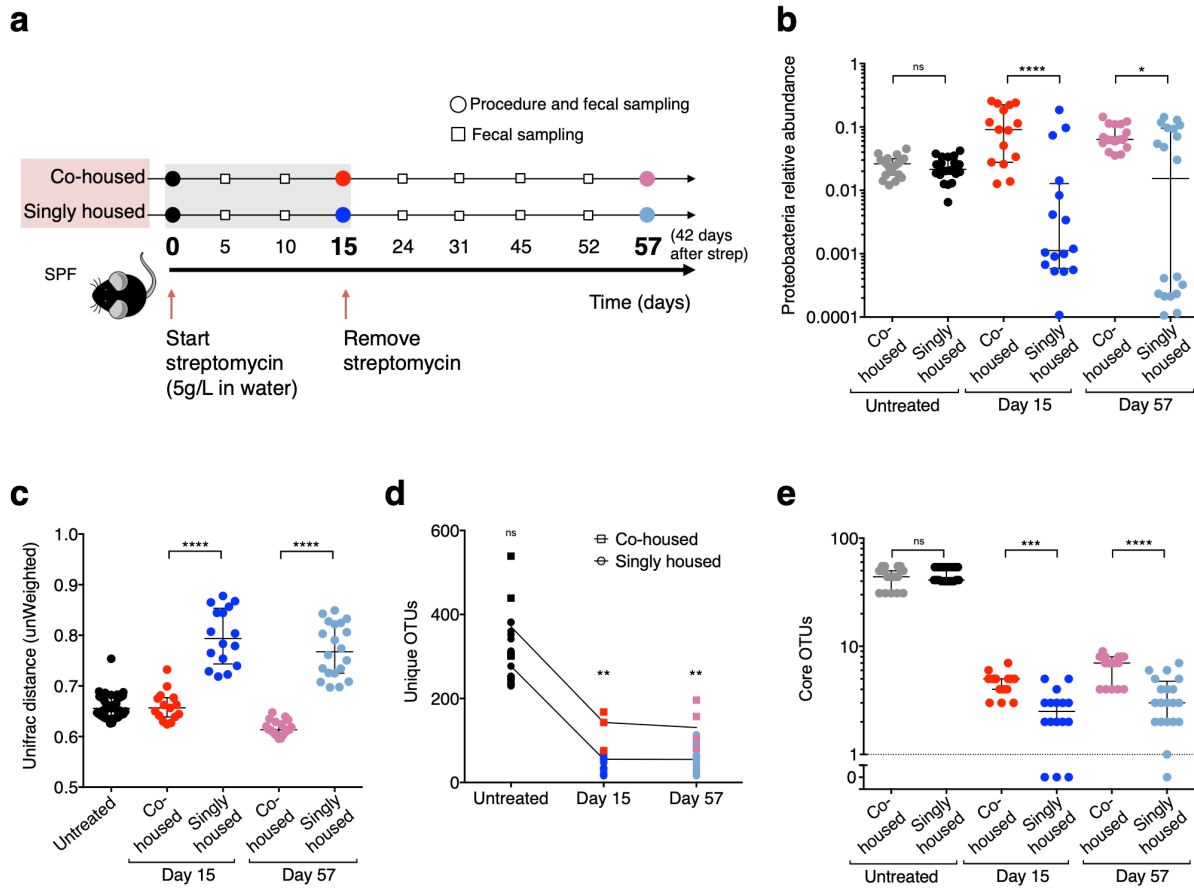


Fig. 1| Streptomycin causes stochastic changes to microbiota composition and a

decrease in diversity in singly housed mice compared with co-housed mice. a,

Experimental scheme for streptomycin treatment and after treatment in 4 independent

mice cohorts (10 to 11 mice each). 5 g/L of streptomycin was administered in the drinking

water to 5 co-housed and 5-6 singly housed SPF C57BL/6J mice on day 0 and removed on

day 15. Fecal samples were collected before (day 0), during (day 15), and after (day 57)

antibiotics for microbiota composition analysis. **b**, Relative abundances of the

Proteobacteria phylum in co-housed and singly housed mice at indicated time points. **c**,

Phylogenetic dissimilarities on each day determined by the mean unweighted Unifrac

distance of the bacterial communities of each mouse to each other mouse within the same group. Data shown are medians, and error bars show interquartile range ($n=20-21$ per group). **d**, Gamma diversity of the gut microbiota of the co-housed and singly housed mice at indicated time points. Lines represent median values ($n=3-4$ cages for co-housed, $n=15-21$ cages for singly housed). **e**, Number of core OTUs (present in every mouse of each group before treatment) at days 0, 15, and 57. Shown are median values, and error bars show the interquartile range across $n=15-21$ per group. Data were analyzed with the Mann-Whitney test (*: $p<0.05$; **: $p<0.001$; ***: $p<0.0001$; ns, not significant).

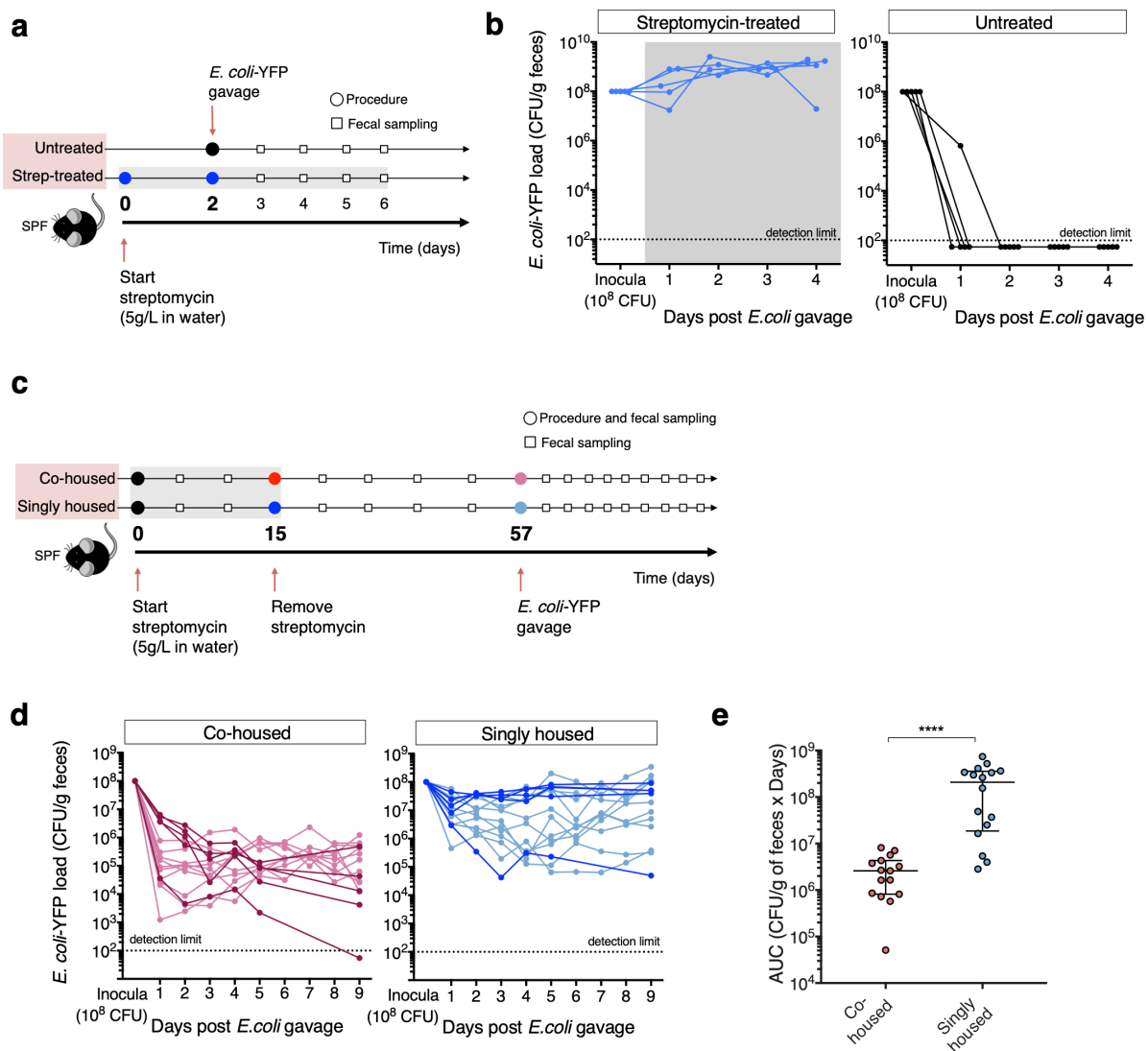


Fig. 2| Co-housed mice are resistant to *E. coli* colonization, unlike most singly housed

mice. a, Experimental scheme for measuring the capacity to resist colonization by *E. coli*. *E.*

coli-YFP cells were orally administrated to cohorts of untreated and streptomycin-treated

mice on day 2. Fecal samples were collected at indicated time points for *E. coli*-YFP

quantification. **b**, Loads of *E. coli*-YFP in CFUs/g feces remained high in streptomycin-

treated mice (grey – streptomycin treatment; left), but became undetectable in untreated

1118 mice by day 1-2 (right). *n*=5 per group. **c**, Experimental scheme for measuring the capacity
1119 to resist colonization by *E. coli* in 3 of the 4 independent cohorts of co-housed and singly
1120 housed mice after streptomycin treatment. *E. coli*-YFP cells were orally administered to all
1121 mice on day 57. Fecal samples were collected for 9 days post gavage for *E. coli*-YFP
1122 quantification. **d**, Loads of *E. coli*-YFP colonization in cohorts 2-4 in co-housed mice (left)
1123 and singly housed mice (right). *n*=15-16 per group. Loads of *E. coli*-YFP in cohort 2 are
1124 shown in dark pink or dark blue. In this cohort loads of *E. coli*-YFP gradually decreased in
1125 co-housed mice (dark pink lines, left), but remained high in all singly housed mice except
1126 mouse 10 (dark blue lines, right). The microbiota composition of cohort 2 was analyzed in
1127 samples from days 0, 15, and 57 of co-housed (Mouse 1-5) and singly housed (Mouse 6-10)
1128 mice (Supplementary Fig. 3). *n*=5 per group in cohort 2. **e**, Area Under the Curve (AUC)
1129 calculated from the dynamics of *E. coli*-YFP CFU/g feces during the experiment for each of
1130 the co-housed and singly housed mice of the 3 cohorts tested in **d**, demonstrating that co-
1131 housed mice had significantly lower loads of *E. coli* throughout the experiment than singly
1132 housed mice. Data in **e**, show medians and interquartile ranges and were analyzed with the
1133 Mann-Whitney test (****: $p < 0.0001$).

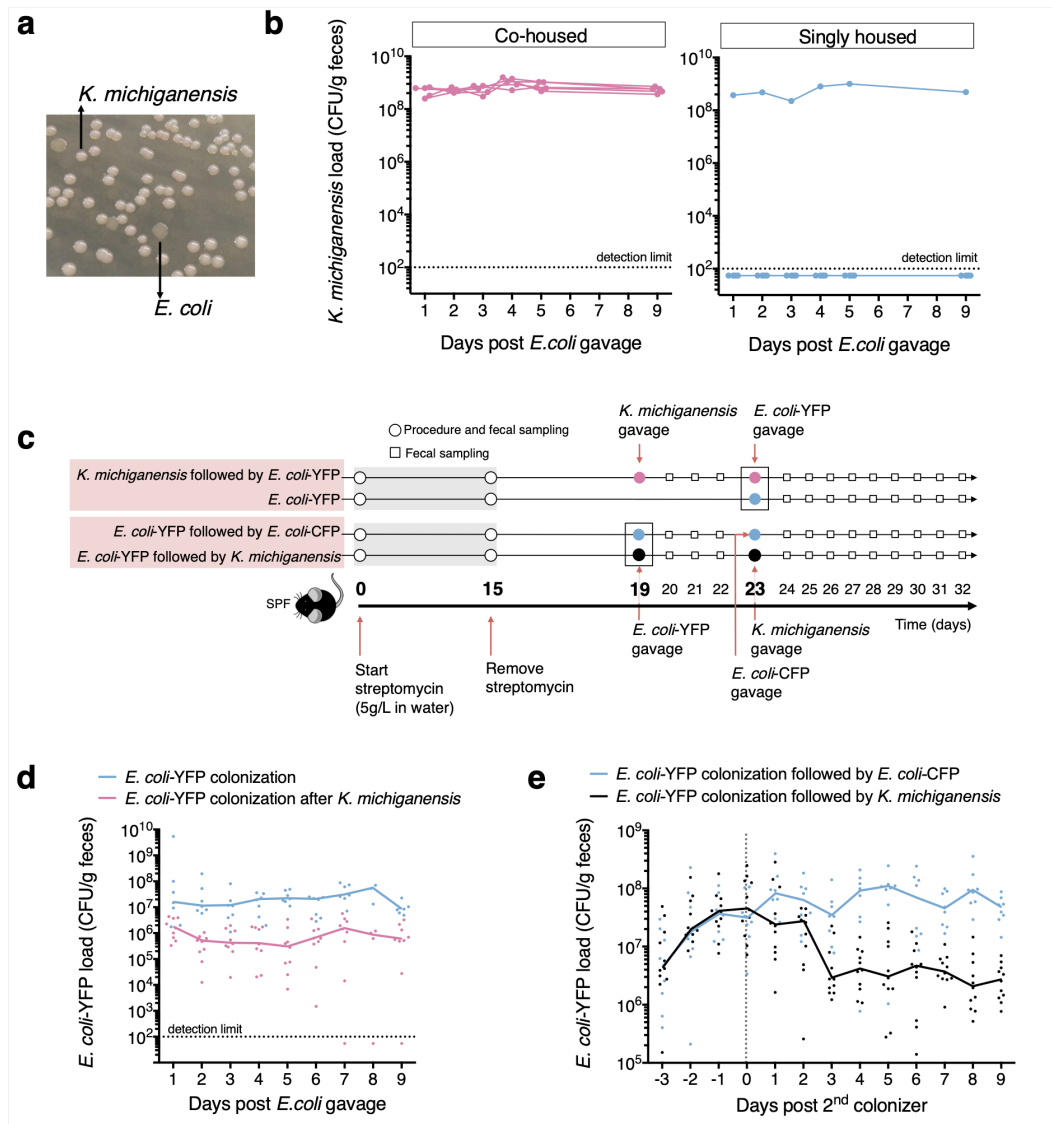


Fig. 3| *K. michiganensis* provides colonization resistance against *E. coli*. **a**, *E. coli* and *K. michiganensis* are easily distinguishable based on colony morphology when grown on LB agar and incubated overnight at 37 °C. **b**, After streptomycin treatment, loads of *K. michiganensis* (CFUs/g feces) of cohort 2 from the experiment in Fig. 2c,d were high in co-housed mice (left), but at undetectable levels in all singly housed mice except one (right). $n=5$ per group. **c**, Experimental scheme for measuring the capacity in singly housed mice of *K. michiganensis* to increase colonization resistance against or displace *E. coli* after

streptomycin treatment. 5 g/L streptomycin was administered in the drinking water starting on day 0 and removed at day 15. Fecal samples were collected before (day 0), during (day 15), and after (days 19, 23, 28, and 32) antibiotics. *K. michiganensis*, *E. coli*-YFP, or *E. coli*-CFP cells were orally administered on indicated days. Fecal samples were collected daily after gavage for *K. michiganensis* and *E. coli* quantification. $n=7-11$ per group. **d**, Loads of *E. coli*-YFP (CFUs/g feces) when colonizing alone were higher than in mice pre-colonized with *K. michiganensis* ($n=7-9$ per group across two independent experiments; comparisons of the different AUC are shown in Supplementary Fig. 5b). **e**, *E. coli*-YFP (CFUs/g feces) colonization before and after challenge with *E. coli*-CFP ($n=8$, across two independent experiments) or *K. michiganensis*. ($n=11$, across three independent experiments). *K. michiganensis* gavage resulted in a substantial decrease in *E. coli* loads (comparisons of the different AUC are shown in Supplementary Fig. 5d). Circles and lines in **d** and **e** represent values from individual mice and medians, respectively.

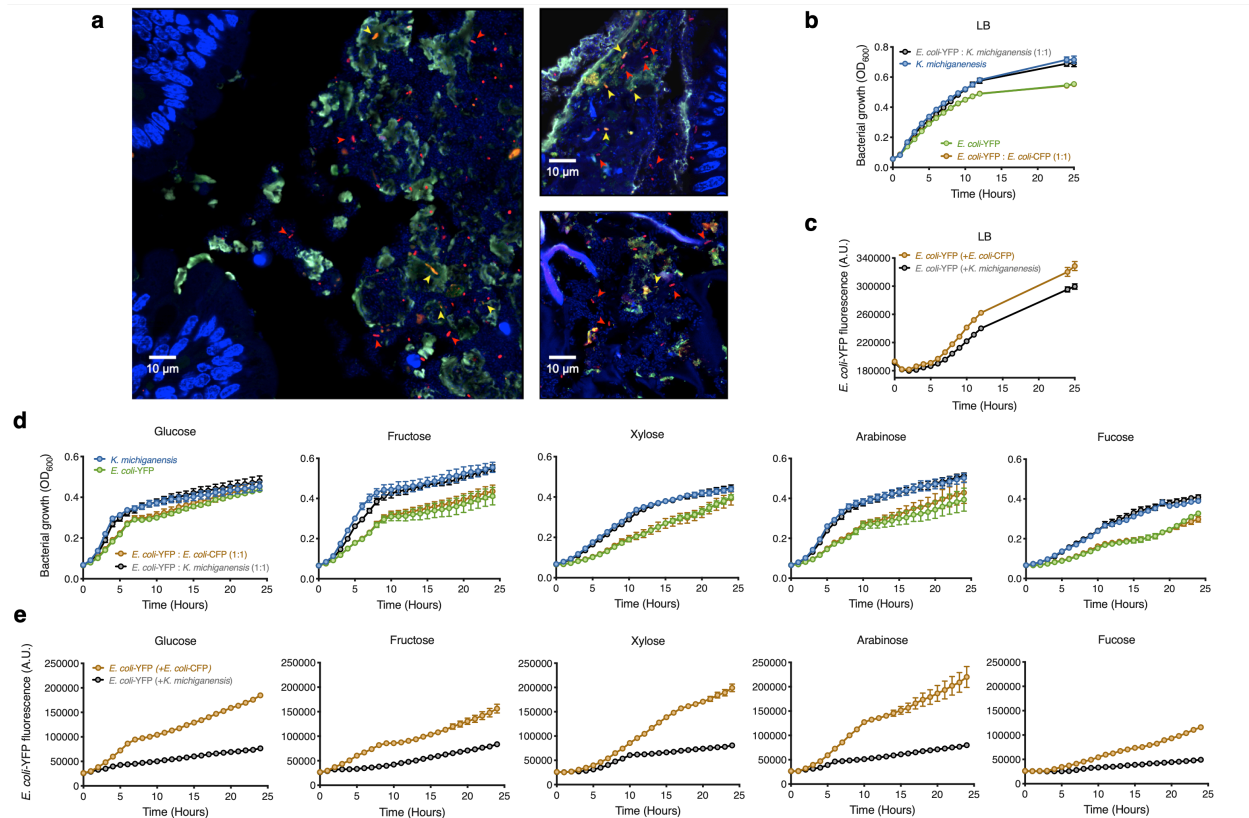


Fig. 4| Competition for simple sugars provides a fitness advantage to *K.*

***michiganensis* over *E. coli*.** **a**, Intestinal sections were stained with 16S rRNA FISH probes targeting Gammaproteobacteria (red) and *E. coli* (green). In the images, *E. coli* (yellow, since cells are targeted with both red and green FISH probes) and *K. michiganensis* (red, targeted only with the Gammaproteobacteria probe) were in close proximity in many regions of the colon of mice colonized with both species, indicating that they inhabited similar spatial niches. Mucus (green) and DNA (blue) were stained with UEA1 and DAPI, respectively. The large, puffy, diffuse green staining is mucus. There were no bacteria-sized objects that appeared only in the green channel; all such green-stained objects were also red-stained and therefore appeared yellow. **b**, Cell density of co-cultures of *E. coli*-YFP with *K. michiganensis* or *E. coli*-CFP showed that *K. michiganensis* has a slight advantage in LB

1167 medium. Growth was monitored by OD₆₀₀ measurements ($n=3$ per condition). **c**, *E. coli*-YFP
1168 growth capacity in LB medium was lower in co-cultures with *K. michiganensis* as compared
1169 with *E. coli*-CFP. *E. coli*-YFP growth was monitored by YFP fluorescence quantification ($n=3$
1170 per condition). **d**, Sugar utilization capacity of *K. michiganensis* and *E. coli* alone or in co-
1171 cultures in minimal media containing 0.25% of the indicated carbon source. Growth was
1172 monitored by OD₆₀₀ measurements every hour for 24 h ($n=6$ curves per condition). *K.*
1173 *michiganensis* generally exhibited faster growth than *E. coli* across all carbon sources. **e**, *E.*
1174 *coli*-YFP growth capacity in co-cultures in minimal media containing 0.25% of the indicated
1175 carbon source. *E. coli*-YFP growth was monitored by YFP fluorescence quantification every
1176 hour for 24 h ($n=6$ per condition). *E. coli* yield was lower when grown with *K. michiganensis*
1177 compared with *E. coli*-CFP across all carbon sources Data in **b-e** represent means and
1178 standard deviations.

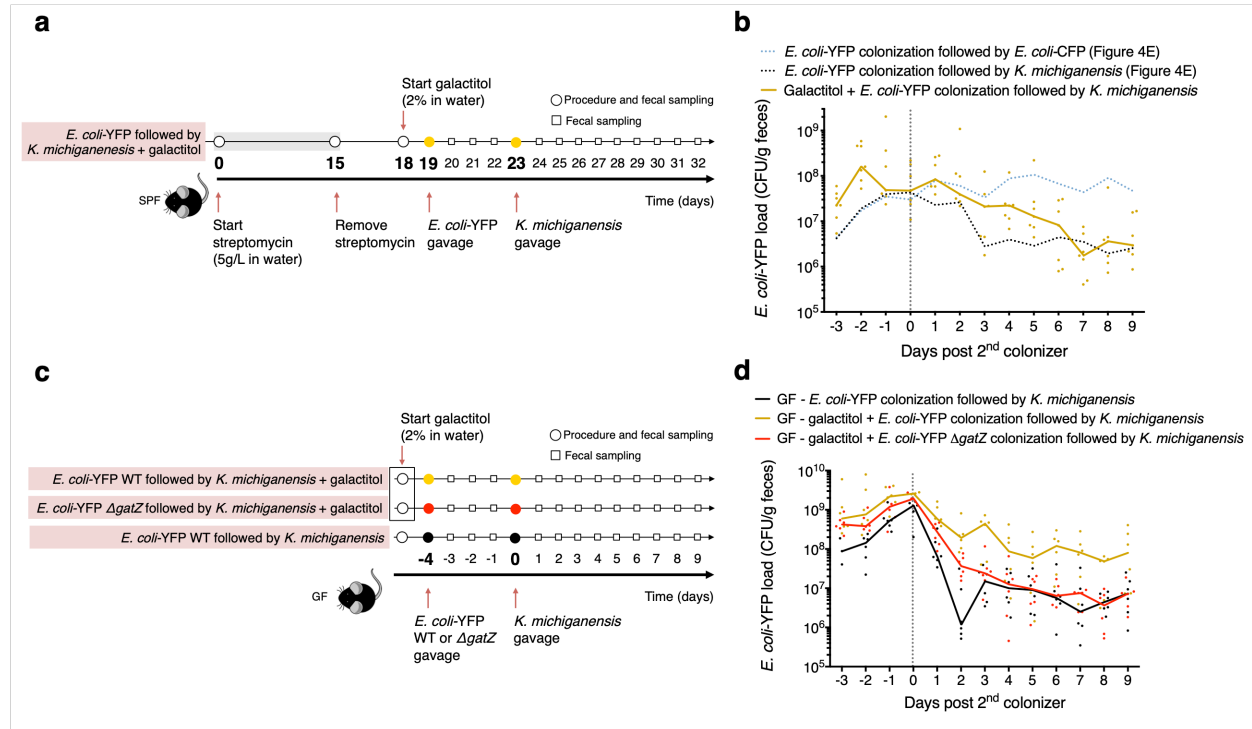


Fig. 5| A nutritional advantage for *E. coli* abolishes the colonization resistance capacity of *K. michiganensis*. **a**, Experimental scheme for measuring the capacity of galactitol to affect *K. michiganensis*-mediated colonization resistance against *E. coli* in singly housed mice after streptomycin treatment. 5 g/L of streptomycin was administered in the drinking water from day 0 to day 15. Fecal samples were collected before (day 0), during (day 15), and after (days 19, 23, 28, and 32) antibiotics. Mice were given water supplemented with 2% galactitol from day 18 onward. *K. michiganensis* or *E. coli*-YFP cells were orally administered on indicated days. Fecal samples were collected daily after gavage for *K. michiganensis* and *E. coli*-YFP quantification ($n=7$). **b**, Loads of *E. coli*-YFP (CFUs/g feces) before and after challenge with *K. michiganensis* in mice with drinking water supplemented with 2% galactitol (yellow dots and line, $n=7$ across two independent experiments). Dashed lines represent median values of CFUs/g feces of *E. coli*-YFP colonization before and after challenge with *E. coli*-CFP (blue) or *K. michiganensis* (black) in

mice without galactitol administration from Fig. 3e, which were performed in parallel with the groups from the two independent experiments that received galactitol, and are shown here for comparison. Galactitol attenuated the colonization resistance against *E. coli*. **c**, Experimental scheme for measuring the capacity of galactitol to affect *K. michiganensis*-mediated colonization resistance against *E. coli* in singly housed gnotobiotic mice. Mice were either given non-supplemented water or water supplemented with 2% galactitol from day 18 onward. *K. michiganensis*, *E. coli*-YFP, or *E. coli*-YFP $\Delta gatZ$ cells were orally administered on indicated days. Fecal samples were collected daily after gavage for *K. michiganensis*, *E. coli*-YFP, and *E. coli*-YFP $\Delta gatZ$ quantification ($n=6$ across two independent experiments). **d**, Loads of *E. coli*-YFP and *E. coli*-YFP $\Delta gatZ$ (CFUs/g feces) before and after challenge with *K. michiganensis* in mice with non-supplemented drinking water or water supplemented with 2% galactitol ($n=6$ across two independent experiments). Galactitol attenuated the colonization resistance against *E. coli*. Circles and lines represent values from individual mice and medians, respectively. For **b** and **d**, comparisons of the different AUC are shown in Supplementary Fig. 7d,f, respectively).

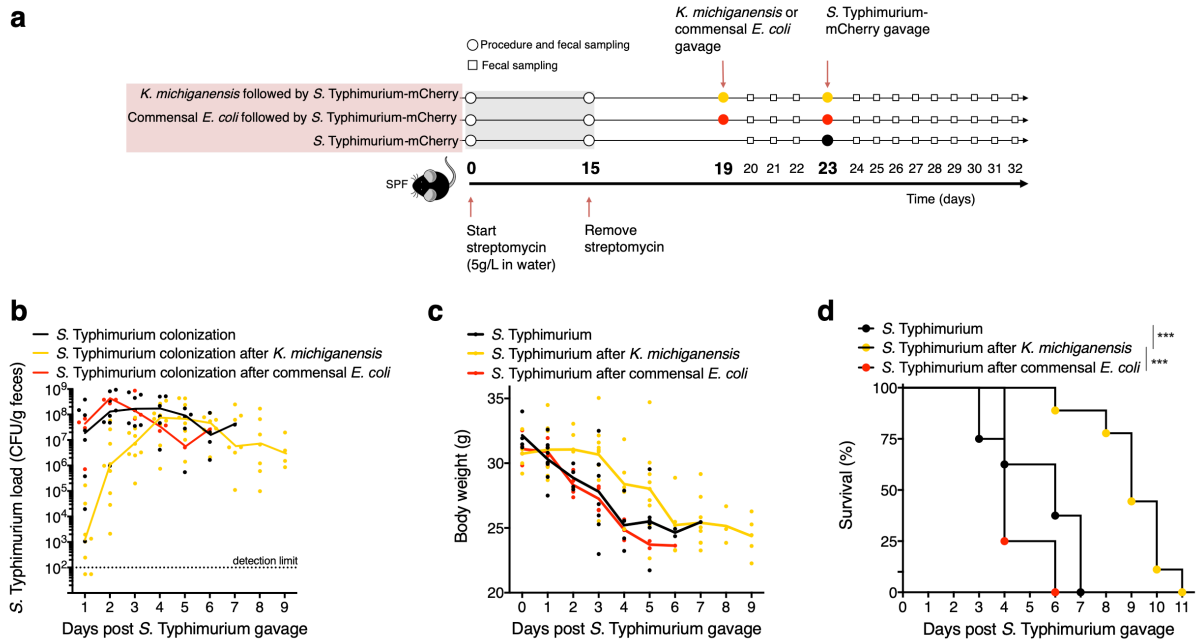


Fig. 6| *K. michiganensis* delays gut expansion of *S. Typhimurium*. **a**, Experimental

scheme for measuring the capacity of singly housed mice to resist colonization by *S.*

Typhimurium after streptomycin treatment. Streptomycin was administered in the

drinking water starting on day 0 and ending on day 15. Fecal samples were collected before (day 0), at the end of antibiotics (day 15), and daily between days 19 and 32. *K.*

michiganensis, commensal *E. coli*, and *S. Typhimurium* were orally administered on

indicated days. Fecal samples were collected daily after gavage for *K. michiganensis*,

commensal *E. coli*, and *S. Typhimurium* quantification ($n=4-9$ per group). **b**, Loads of *S.*

Typhimurium (CFUs/g feces) increased more slowly in mice pre-colonized with *K.*

michiganensis ($n=9$ across two independent experiments), as compared to mice not pre-

colonized or pre-colonized with a commensal *E. coli* ($n=8$ across two independent

experiments and $n=4$ in one independent experiment, respectively). **c**, Body-weight loss

due to *S. Typhimurium* infection was delayed in mice pre-colonized with *K. michiganensis*.

d, Mice infected with *S. Typhimurium* exhibited extended survival when pre-colonized with

1223 *K. michiganensis* (*: $p < 0.05$, Log-Rank (Mantel-Cox) test, $n = 4-9$ per group). Circles and lines
1224 in **b,c** represent values from individual mice and medians, respectively. For **b**, comparisons
1225 of the different AUC are shown in Supplementary Fig. 8b).